Engineering Applications of Artificial Intelligence 116 (2022) 105490

Contents lists available at ScienceDirect

Engineering Applications of Artificial Intelligence

journal homepage: www.elsevier.com/locate/engappai

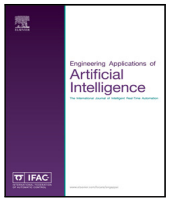

Survey paper

Recent advancements in deep learning based lung cancer detection: A systematic review

Shubham Dodia [a,*], Annappa B. [a], Padukudru A. Mahesh [b]

[a] Department of Computer Science and Engineering, National Institute of Technology Karnataka, Surathkal, India
[b] Department of Respiratory Medicine, JSS Medical College, JSS Academy of Higher Education and Research, Mysuru, Karnataka, India

ARTICLE INFO

Keywords:
Lung cancer
Deep learning
Nodule detection
Medical imaging
Computed Tomography

ABSTRACT

Cancer is considered to be a key cause of substantial fatality and morbidity in the world. A report from the International Agency for Research on Cancer (IARC) states that 27 million new cases of cancer are expected before 2030. 1 in 18 men and 1 in 46 women are estimated to develop lung cancer over a lifetime. This paper discusses an overview of lung cancer, along with publicly available benchmark data sets for research purposes. Recent research performed in medical image analysis of lung cancer using deep learning algorithms is compared using various technical aspects such as efficiency, advantages, and limitations. These discussed approaches provide insight into techniques that can be used to perform the detection and classification of lung cancer. Numerous techniques adapted in the acquisition of the images, extraction of relevant features, segmentation of region affected, selection of optimal features, and classification are also discussed. The paper is concluded by stating the clinical, technical challenges and prominent future directions.

1. Introduction

There are different lung diseases that affect in different parts of thoracic/lung region. Few of the lung diseases that affect the airways of the lung region are asthma, Chronic obstructive pulmonary disease (COPD), chronic bronchitis, emphysema, acute bronchitis, and cystic fibrosis. Lung diseases occurring in the alveoli region of the thoracic region are pneumonia, tuberculosis, pulmonary edema, lung cancer, acute respiratory distress syndrome, and pneumoconiosis. The disease affecting the interstitium region of the lung is interstitial lung disease (ILD). The diseases affecting the blood vessels are pulmonary embolism (PE), and pulmonary hypertension. The diseases that affect the pleura region of the lung are pleural effusion, pneumothorax and Mesothelioma. The diseases that affect the chest wall are obesity hypoventilation syndrome and neuromuscular disorders. Based on the region affected, different diseases occurring in the lung can be bifurcated. In this work, the focus is given to the lung cancer identification using deep learning methods.

Cancer is considered to be the world's most life-threatening illnesses. Many types of cancer affect men and women alike. The medical term referring to uncontrolled and irregular growth of cells in any tissue causing lumps, nodules, or masses to develop is known as cancer (Rajan et al., 2019). Over 100 cancer types can occur in various tissues such as breast, skin, lung, colon, prostate, blood, among others (Tran et al., 2019). In many situations, there are no unique symptoms suggestive of cancer, and thus the diagnosis may be delayed without a high degree of suspicion. The following symptoms are often seen in cancer patients. They are non-specific, such as frequent respiratory infections, shortness of breathing, reduced desire to eat, fatigue, weight loss, pain, pattern changes on the skin, bowel or bladder function changes, abnormal bleeding, constant cough or speech changes, fever, lumps, or masses.

Cancer staging is related to the magnitude of cancer spread. It is often determined by a combination of various imaging techniques and relevant tissue biopsy, which is helpful in identifying the type of cancer. Staging is relevant for the prognosis, where it helps caregivers determine therapy protocols, which may include chemotherapy, immunotherapy, radiation, and surgery either alone or in various combinations. In particular, cancer in the body is more aggressive in later staging, i.e., the higher the stage (generally between 0 and 4), critical the patient's condition. These treatments vary according to stage and type of cancer.

The human body retains cell growth and regenerates whenever necessary. But in unusual conditions, cell growth is uncontrolled and creates the cell clusters called a tumor. Tumors can be categorized into two types, non-cancerous and cancerous. Non-cancerous tumors are benign tumors, and cancerous tumors are malignant tumors. It is possible to treat and remove the benign tumor as it does not invade other tissues or organs. Benign tumors can be completely treated by surgery. There is a maximum possibility that it will not reoccur, and if it does, it will occur in the same place. Whereas a malignant tumor

* Corresponding author.
E-mail addresses: shubham.dodia8@gmail.com (S. Dodia), annappa@ieee.org (Annappa B.), mahesh1971in@yahoo.com (P.A. Mahesh).

https://doi.org/10.1016/j.engappai.2022.105490
Received 26 June 2022; Received in revised form 18 August 2022; Accepted 27 September 2022
Available online 7 October 2022

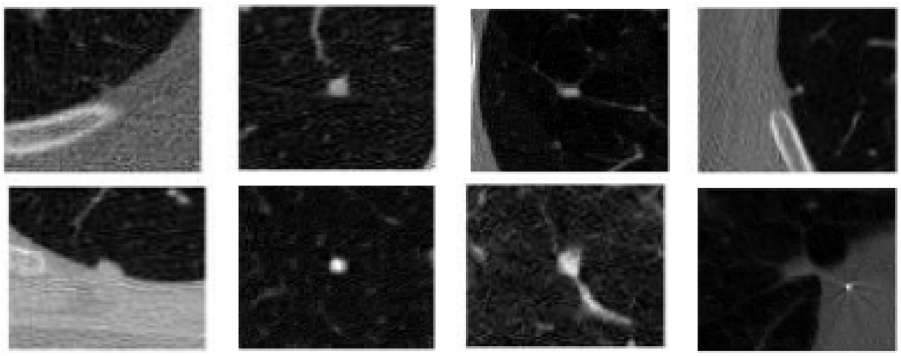

Fig. 1. Different types of nodules. Column-wise: 1. Juxtapleural; 2. Well-Circumscribed; 3. Vascularized and 4. Pleural-tail.

can be treated using chemotherapy, radiation therapy, etc. But these tumors may reoccur and has a high chance of invading other tissues and organs (Sinha, 2018).

Notably, there is a decrease in mortality rate in the developed countries as there is an improvement in the identification, detection in early stages, diagnosis, and treatment of the disease. Tissue biopsy is an image-guided procedure to identify whether a nodule detected is malignant or benign. Studies have shown that the mortality rate is high for many patients diagnosed in the later stages (Chiang et al., 2019). There has been a growing trend in the identification of lung cancer at earlier stages over the last two decades. Initially, chest X-ray screening was studied, but it was not successful in early detection as many subjects had interval lung cancer. It also failed to show a decrease in the mortality rate (Kvale et al., 2014). Low dose Computed Tomography (CT) scans have been recently tested as means for lung cancer detection (Sverzellati et al., 2016; Robles and Harris, 2017; Choi et al., 2018). The key questions to be addressed are how effective screening is of large-scale at-risk populations for early diagnosis of lung cancer and how sensitive and accurate are image findings for lung cancer diagnostics.

The development of an irregular circular/oval growth in the lungs called lung nodules is regarded as an early manifestation of lung cancer. The complex lung structure makes the diagnosis of lung cancer a tedious task (Lavanya and P., 2018). As explained by Kuruvilla and Gunavathi (2014), radiologists categorize nodules into four different types, such as Juxtapleural, Well-circumsized, Vascularized, and Pleural-tail. This can be illustrated in Fig. 1 (Farag et al., 2010).

Size is a primary determinant of a nodule, whether it is a benign or malignant nodule. A lung nodule greater than 3 cm in size has a higher risk of being malignant (Choromańska and Macura, 2012). The "doubling time" is even more significant, which is the time taken for the nodule volume to double. This is a more sensitive and specific feature of malignant lesions than just the size, but it needs serial images, i.e., images taken in the previous check-ups, in order. If the doubling time is faster, i.e., it is less than 30 days; it is likely to be due to a benign cause such as an infection. A lesion that stays static for two years is considered benign.

Numerous imaging techniques are used for the diagnosis, classification, and recognition of stages of lung cancer. Some of the popular techniques are CT, Magnetic Resonance Imaging (MRI), Positron Emission Tomography (PET), chest radiograph (popularly known as X-ray), etc. These imaging techniques provide local information on the presence of a tumor, metastate of the presence of the disease, and even the lymph nodes in the human body. A combination of imaging techniques such as PET and CT is also made to get deeper anatomical information of the region. Computer-Aided Diagnosis (CAD) devices are used to identify lung nodules automatically, which allow radiologists to detect disease. The details regarding the imaging modalities are given in Image Acquisition section.

Multimodal learning is a technique which is a combination of two or more modalities and can be performed in two different ways. Firstly, multimodal learning is done using combination of different imaging modalities. The modalities include popular techniques such as CT, X-ray, PET, MRI etc. The most used multimodal learning is PET/CT combination (Kao and Yang, 2022; Qin et al., 2020; Shi et al., 2020). The combination of the imaging modalities is quite a tedious task as the data dimension and the annotation style are different for each modality. There is still a lot of future scope to work in the combination of different imaging modalities and overcome these issues. Secondly, multimodal learning can be done using combination of different feature extraction techniques with clinical data of the patients. Many features can be extracted using clinical data by analyzing the physical characteristics of the patients over the span of years. Image-based features can be extracted using different image processing techniques from the CT scans. The combination of these two sets of features are used for lung cancer nodule detection (Kumar et al., 2019; Huang et al., 2020; Nazir et al., 2021). In the past few years, self-supervised learning techniques have been in the trend for medical imaging data. There are some works that have used deep learning self-supervised architectures for image demonizing (Lei et al., 2021) and nodule detection (Liu et al., 2019a). However, this domain still needs to be explored.

A survey published by Mahesh et al. reveals that the age-adjusted incidence rate of lung cancer varies from 7.4 to 13.1 per 100,000 males and between 3.9 and 5.8 per 100,000 females in India (Mahesh et al., 2012). About 70% of the patients are detected with lung cancer at their final stages, and only 16% have a chance of surviving in the next five years states (Kulkarni and Panditrao, 2014). According to Baldwin (2015), if the patients are diagnosed earlier, there are 70% chances of improving the survival rate till five years. As mentioned earlier, lung carcinoma or lung cancer is a cause of many deaths in cancer around the world, with a death rate of 19.5% and a prevalence of 13% across all cancers (Ferlay et al., 2015; Bhavanishankar and Sudhamani, 2015). During 2017, lung cancer estimated around 26% of all deaths from cancer, affecting more than 1.5 million deaths worldwide (da Nóbrega et al., 2018). The World Health Organization (WHO) states that cancer accounted for an expected death of 9.6 million in 2018, and globally, cancer causes about 1 in 6 deaths (Ferlay et al., 2015). In 2022 only in United States, according to estimates by American Cancer Society, there will be an estimated total of 1.9 million new cancer cases identified and 609,360 cancer deaths, or roughly 1670 deaths every day. Out of the 17.2 million cancer cases reported in 2016, there were 8.9 million deaths. A work published by Shaziya et al. (2018) states that about 1.69 million deaths have been caused by lung cancer throughout the year 2015. Lung cancer ranked the highest position among other cancers worldwide in 2018 based on incidence and mortality. This constitutes 11.6% of all cases of cancer and 18.4% of all deaths from cancer (Bray et al., 2018). It is reported in the National Cancer Registry of China that the number of deaths caused by cancerous tumors in China has reached 5,91,000 in the year 2016. The casualties include both males (4,02,000) and females (1,89,000), which sums up to 26.51% of deaths from cancerous tumors alone. The overall mortality

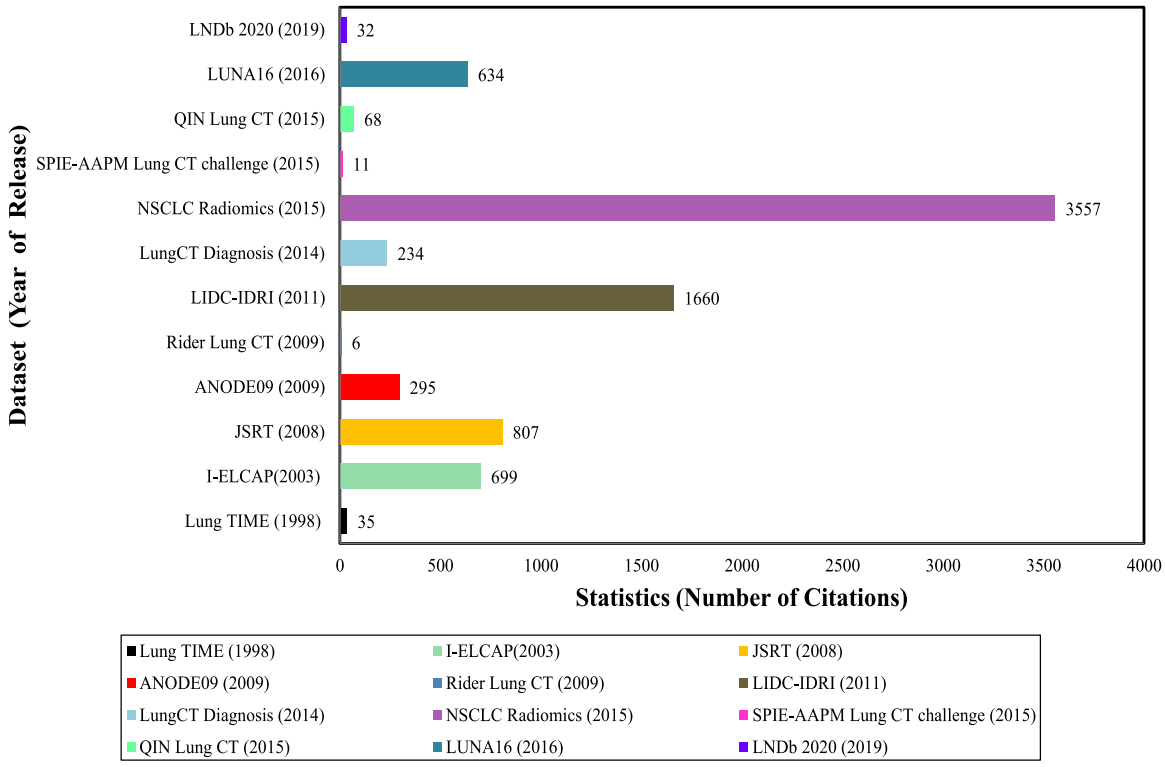

Fig. 2. Statistics of the dataset usage in the existing literature.

rate for lung cancer was 43.41/100,000, which includes 57.64/100,000 males and 28.45/100,000 females (Liu et al., 2019b). Approximately 20% of all cancer mortalities are caused by lung cancer (Bhalerao et al., 2019). Also, there were 21 million new cases and 1.8 million deaths reported in Bhalerao et al. (2019) for 2018 alone. Roughly, 1,42,670 lung cancer deaths (76,650 in men and 66,020 in women) are expected in the United States by the American Cancer Society for 2019 (DeSantis et al., 2019).

2. Datasets

The availability of datasets plays a crucial role in the automation of lung cancer nodule detection and classification. To attain reliable performance results using computational techniques, dataset is a necessary requirement. There are some publicly available datasets for detection, identification, and classification of lung cancer nodules. Lung cancer detection involves distinguishing nodules and non-nodules in the lungs, whereas, classification task is separating non-cancerous nodules and cancerous nodules in the lungs. Table 1 provides information about available datasets on lung cancer. The table contents include the dataset name, date of release, number of samples, size of the dataset in gigabytes, the total number of images, image modality, image dimension, the format in which the images are stored, and ground truth availability. The table lists the datasets available and is chronologically arranged on the basis of the release date.

The statistics of the dataset usage in the existing literature is depicted in Fig. 2. The graph is plotted on the basis of the citations received for the dataset according to google scholar statistics. The references cited for each dataset are given in the respective website portal and/or the challenge organizers.

3. Generalized lung cancer detection system

The framework is basically divided into conventional/traditional and deep learning algorithms. The traditional architecture mostly consists of various steps, including preprocessing, segmentation, nodule candidate generation, feature extraction, feature selection, and classification. However, some steps from the above mentioned can be optional based on the requirement. In deep learning, the input provided to the network is an input image, and the model learns the representation of the feature from the input image. An architecture of a generalized lung cancer detection system on conventional approaches is illustrated in Fig. 3, and a deep learning architecture is illustrated in Fig. 4. Further description of the steps involved is discussed in the sub-sections below.

3.1. Image acquisition

Acquiring images from various imaging techniques is the first step carried out in a CAD model. Data acquisition is a process of capturing images by systematically scanning the patient. There are multiple modalities for performing image acquisition, which includes chest radiograph, magnetic resonance imaging, and computed tomography scans. The imaging techniques used for capturing the chest/thoracic region are illustrated in Fig. 5. Three imaging modalities are shown, namely, chest X-rays, MRI, and CT scan.

The first test that is usually conducted for lung cancer diagnosis is a chest X-ray. Chest radiographs are known to be one of the earlier imaging techniques. Lung cancer is identified as a white–gray mass in an X-ray image. The drawback of using X-rays for lung cancer diagnosing lung cancer is that a definitive diagnosis is not provided. The reason is that from X-ray images, it is difficult to discriminate between lung abscess and cancer condition. Therefore, after an X-ray, doctors suggest another scan or test for confirming the presence of lung cancer. The second technique for acquiring images of the lung is MRI. This technique also generates images that allow doctors to see the location of a lung tumor and measure the size of the tumor. MRI produces more detailed images as compared to X-ray images as the images are captured using magnetic fields. A special dye named contrast medium is given to the patient to get a clearer image before undertaking the scan. But, there is a drawback of using MRI for lung

Table 1
Available datasets for medical image analysis of lung cancer.

Dataset	Date of release	Dataset size (GB)	Number of samples	Number of images	Image modality	Image dimension	Image format	Ground truth availability
Lung TIME (Dolejsi et al., 2009)	1998	18.9	157	N/A*****	CT*	N/A	DICOM	Yes
I-ELCAP (Fontana et al., 1986)	2003	4.76	50	N/A	CT	N/A	N/A	Yes
JSRT (Shiraishi et al., 2000)	2008	2.05	247	N/A	X-ray	2048 × 2048	IMG	Yes
ANODE09 (Ginneken et al., 2010)	2009	5.61	55	N/A	CT	512 × 512	Meta	Yes (For training set only)
Rider Lung CT (Zhao et al., 2015)	2009	7.55	46	15,419	CT	N/A	DICOM	Yes
LIDC-IDRI (McNitt-Gray et al., 2007)	2011	124	1018	2,44,527	CT, DX**, CR***	512 × 512	DICOM	Yes
LungCT Diagnosis (Grove et al., 2015)	2014	2.5	61	4682	CT	N/A	DICOM	Yes (For tumor sizes only)
NSCLC Radiomics (Aerts et al., 2014)	2015	725	422	51,513	CT, RSTRUCT****	N/A	DICOM	Yes
SPIE-AAPM Lung CT challenge (Armato et al., 2015)	2015	12.1	70	22,489	CT	N/A	DICOM	Yes
QIN Lung CT (Morris et al., 2018)	2015	2.27	47	3954	CT	N/A	DICOM	No
LUNA16 (Setio et al., 2017)	2016	116	888	N/A	CT	512 × 512	DICOM	Yes
LNDb 2020 (Pedrosa et al., 2019)	2019	N/A	294	N/A	CT	N/A	DICOM	Yes

CT*-Computed Tomography DX**-Digital Radiography CR***-Computed Radiography RTSTRUCT****- RadioTherapy STRUCTure set N/A*****-Not Available.

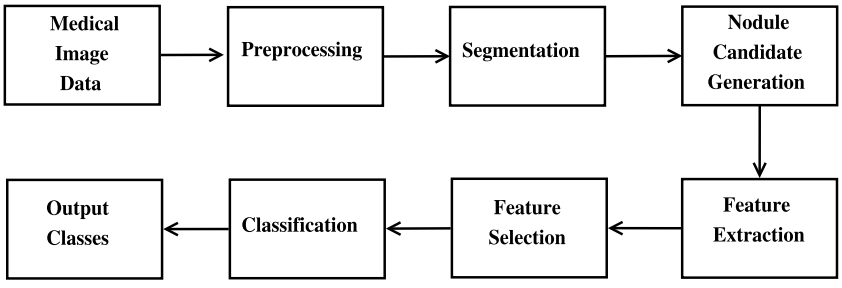

Fig. 3. Conventional machine learning based CAD system for Lung Cancer.

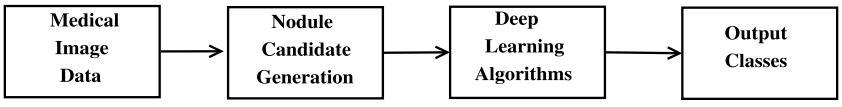

Fig. 4. Deep Learning based CAD system for Lung Cancer.

cancer diagnosis. MRI scanning does not work well for body parts that are in motion, such as lungs. It moves every time a person breathes. Therefore, to detect lung cancer, MRI scanning is rarely used.

The most effective imaging technique used in recent trends is the CT scan. This scan is usually conducted after doctors have taken X-rays and recommend for confirmation of the presence of lung cancer

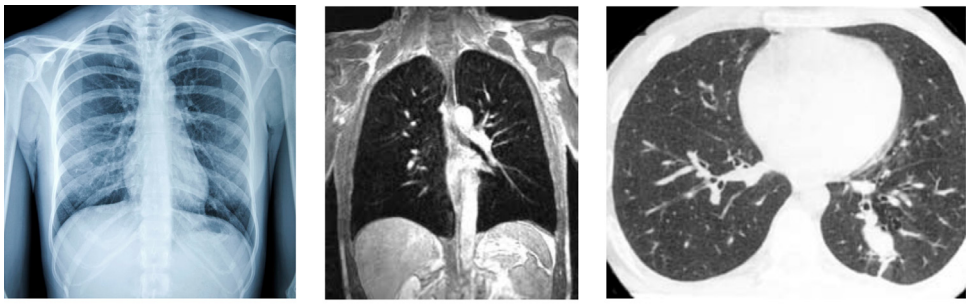

(a) Chest Radiograph (X-ray) (b) Magnetic Resonance Imaging (MRI) (c) Computed Tomography (CT)

Fig. 5. Different imaging modalities used for capturing details of chest/thoracic region.

tumors. CT scan is painless and takes 20–30 min for the complete scan. A beam geometry of the third generation, which is the most common geometry, is determined by coupling and is used in CT systems. During the scanning process, X-ray tube and detectors keep revolving around the patient to capture multiple slices (Seeram, 2010).

3.1.1. Why CT is preferable?

Lung cancer can be diagnosed in the early stages using CT images. Many CAD systems use CT scanning because the process of image capture is quick and does not damage the patient's bones, and is less noisy (Potghan et al., 2018). Imaging tests like CT scans can recognize lung cancer as it provides a more accurate picture (Kulkarni and Panditrao, 2014). CT scan is said to be more powerful in identifying and diagnosing lung cancer than regular chest X-rays. Using CT scans, a 3-dimensional image can be reconstructed as the images' acquisition is performed in a continuous manner (Hollings and Shaw, 2002). Scanning CT is the most suitable method to visualize lung cancer (Niranjana and Ponnavaikko, 2017). As per Lakshmanaprabu et al. (2019), CT is best suited for tracking the location of tumors and determining the stage of cancer in the body. CT scanning is used to identify lung mass tissue or nodules because it can detect very minute irregularities that suggest lung cancer (Aggarwal et al., 2015).

In medical practice, the most powerful and common imaging technique is CT for detecting nodules and for the diagnosis with benefits such as cost-effectiveness, high spatial resolution, availability, and non-invasiveness (Gibaldi et al., 2015; Ng and Goh, 2010). In comparison to PET and MRI imaging techniques, CT is much easier, less costly and can achieve better sensitivity in lung nodule detection than X-ray imaging (Bhavanishankar and Sudhamani, 2015; Cieszanowski et al., 2016). A lung cancer diagnosis at initial stages has shown significant and encouraging results in CT screening in the form of pulmonary nodules, thereby mitigating mortality rate (Monkam et al., 2019). Therefore, most work in this field has been dedicated to lung nodule identification through CT scans of the thoracic region.

However, utilizing the CT modality has several disadvantages, such as radiation exposure levels that frequently approach and occasionally exceed may increase the risk of cancer. In spite of CT scans being speedy, comfortable, and in most cases secure, there is a very small chance that the contrast dye used will cause an allergic reaction.

3.2. Image preprocessing

Acquired data consists of noise due to various reasons. The images captured from the imaging modalities are of low-resolution. In order to improve the quality of the image, the preprocessing stage is important suggests (Thabsheera et al., 2019). The importance of preprocessing images is demonstrated in Fig. 6 (Firmino et al., 2014). The preprocessing steps involve removing noise, improving the image quality by increasing the contrast and brightness of the image etc.

There are several methods involved in preprocessing an image. Some of the methods improvise the image quality by using filters, remove noise from the image, and segment only one region of the lungs from a CT slice (Niranjana and Ponnavaikko, 2017). Most used methods for preprocessing images include: median filters (John and Mini, 2016; Lakshmi Narayanan and Jeeva, 2015; Sivakumar and Chandrasekar, 2013), histogram equalization (Nemade, 2016; Javaid et al., 2016), Gaussian filter (Vignesh and Kothavari, 2014; Novo et al., 2015), Gaussian filter laplacian (LOG) (Fotin et al., 2009; Diciotti et al., 2008), Wiener filter (Nair and D., 2016), Mean filter, Adaptive median filter, Guided filtering (Thabsheera et al., 2019) and combined processes. The above mentioned image preprocessing techniques are described in Table 2.

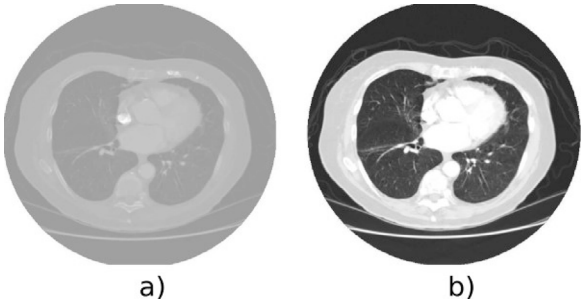

Fig. 6. Demonstration of preprocessing of a chest CT scan. (a) Original image, (b) Preprocessed image in which the artifacts are removed by applying filters and increasing contrast of the image to achieve better quality.

Based on the analysis, Wiener filter is considered to be the best filter to remove noise from the CT scans as it minimizes the overall mean square error in the process of inverse filtering and noise smoothing. The second best performing filters include mean, and adaptive median filter for denoising CT images.

3.3. Image segmentation

Preprocessing the image reduces the noise/artifacts present in an image which makes it easy for further processing. Segmentation step is the process of grouping the pixels based on particular criteria. A series of segments that capture a complete image or a set of contours of an image as a whole is the outcome of image segmentation (Al-Tarawneh, 2012). Segmentation of thoracic region (lungs) is a tedious task as there is no uniformity, and it also provides similar values for pulmonary structures such as lungs, bronchi, bronchioles, and nerves (Niranjana and Ponnavaikko, 2017). Segmentation techniques are categorized into various broad categories. Table 3 discusses the various segmentation methods and their working used in the literature.

3.4. Candidate nodule generation

The next step of a CAD system in which the information of the image is scanned fastly for any potential anomaly locations is known

Table 2
Comparison of various image preprocessing techniques.

Reference	Method	Description
John and Mini (2016), Lakshmi Narayanan and Jeeva (2015), Sivakumar and Chandrasekar (2013)	Median filter	The median filter is a non-linear digital filtering technique, often used to remove noise from an image or signal.
Nemade (2016), Javaid et al. (2016)	Histogram equalization	The histogram equalization is an image processing which enhances the contrast of the image.
Vignesh and Kothavari (2014), Novo et al. (2015)	Gaussian filter	Gaussian filter is a type of linear smoothing filter, in which the weights of the filter are chosen on the basis of Gaussian function.
Fotin et al. (2009), Diciotti et al. (2008)	Laplacian of Gaussian	Laplacian of Gaussian filters are used for detecting edges in the image and also remove noise by smoothening image using Gaussian filter.
Nair and D. (2016)	Wiener filter	Wiener filter is a noise diminishing algorithm in either time or frequency domain. It minimizes mean squared error between the pixels in the image.
Thabsheera et al. (2019)	Mean filter	Mean filtering is a technique where the intensity deviation of one pixel and its successor pixel is decreased using arithmetic mean.
Thabsheera et al. (2019)	Adaptive median filter	An adaptive median filter removes noisy pixels from an image by discriminating the pixels as corrupted and uncorrupted. The filter is applied only on the corrupted pixel window.
Thabsheera et al. (2019)	Guided filtering	The guided filtering technique is a method which performs image smoothing by using the content of a second image and also preserves edges in the image.

as candidate generation, whereas to assess the most likely or important of them, the consecutive stages of the CAD system refines the list of candidates. A list of locations is generated by the candidate generator, and a size estimate is given for each candidate. The candidate generator's primary objective is to reduce search space for the nodule without missing nodules. If such a generator is deficient (gives a huge number of false positives), the time of a model will be increased, and efficiency will be decreased (Fotin et al., 2019).

3.5. Feature extraction

The process by which input data is transformed into a number of specific features is called extraction of features (Kulkarni and Panditrao, 2014). Features can be based on texture, gradient, spatial, histogram, radiomics, and geometrical properties of an image. Some of the texture features include entropy, contrast, energy, homogeneity, etc. Some of the histogram features include skewness, standard deviation, average, etc. Gradient features include the average, kurtosis, standard deviation, etc. Radiomics features can be used in discrimination of benign and malignant nodules. These features help to quantify the nodule's intensity, shape, and texture (Choi et al., 2018). Eventually, information on the position of the nodule is obtained from spatial features (Niranjana and Ponnavaikko, 2017). Some of the geometrical features include area, solidity, equivalent diameter, spherical disproportion, perimeter, roundness, circularity, eccentricity, centroid, and convex-area (Aggarwal et al., 2015). The detailed description of the above mentioned feature representation is given in Table 4.

3.6. Feature selection

The selection of features is a common approach in informatics to minimize data dimensionality (Shin et al., 2019). In terms of data sets, this method is extremely useful as a huge amount of features are extracted, and in some cases, few features are redundant. These redundant features deplete the model's performance by overfitting the data. The feature selection algorithms can be categorized into similarity-based feature selection, sparse learning-based feature selection, and statistical-based feature selection methods illustrated in Fig. 7. Similarity-based feature selection picks the features that maintain similarity. Some of the techniques that are come under similarity-based feature selection are Fisher score, ReliefF algorithm, and trace ratio. Sparse learning-based feature selection methods consist of regularizers such as L1 and L2. Some of the variants of sparse learning-based feature selection methods are R-value based feature selection (RFS) and the LLL21 algorithm. Statistical feature selection picks features based on the standardized test statistics. Some of the techniques used for the selection of features are Analysis of variance (ANOVA), F-score, T-score, DESeq2, and negative binomial distribution algorithm.

3.7. Classification

Classification is a learning approach in which the program is trained to differentiate between two or more classes using input data. The classifier predicts an unknown or new sample of data during the test phase. This approach is beneficial for the medical analysis of lung cancer nodules. It helps in differentiating a nodule and a non-nodule in the lungs region. Also, the nodule can be further classified into a benign and malignant nodule. These results help radiologists and pulmonologists to detect nodule with better confidence.

In general, classification algorithms can be further categorized into two types, namely, machine learning (i.e., traditional/conventional) and deep learning-based. Conventional approaches are automated learning algorithms that use hand-crafted feature representations derived from the input data to classify two classes and predict future samples for unseen data. However, deep learning approaches do not require hand-crafted feature representations because they learn the feature from the given input data. Features that provide better generalization are used for training the deep learning model. Deep learning approaches are in the trend and are performing well in many applications. This approach works very well for a large amount of data and performs better with the increase in data size. This is not the case in conventional algorithms. The conventional algorithms or also the traditional machine learning algorithms reach a saturation in the performance where no further improvement is observed. However, deep learning is data-driven and the performance of the deep models increases when trained on larger amounts of data. This scenario is not observed in traditional algorithms as they tend to stop learning after reaching a certain point (Schmidhuber, 2015).

Various selected algorithms are mentioned in both the categories. The results obtained in various applications such as medical imaging, emotion recognition, speech domain, etc. in recent years have

Table 3
Segmentation techniques along with their working explained.

Segmentation techniques	Working explained
Region Growing	A straightforward way of segmenting images based on regions is region growth. Given that it chooses initial seed locations for picture segmentation, it is also categorized as a pixel-based technique. This method of segmentation focuses at the surrounding pixels of the original seed points and decides if they should be included in the region. Partitioning an image into regions is the primary objective of segmentation.
Spheri-cal/Ellipsoidal Model Fitting	An efficient supervised segmentation algorithm for fitting ellipses to three-dimensional images. FitEllipsoid uses the approach of asking the user to select a few locations in 3D on the object's boundary, after which the plugin constructs an ellipsoid that roughly passes through them.
Discriminative Classifiers	Steps followed by the discriminative method of segmentation are pre-processing, feature extraction, classification and post-processing steps. 1. Noise removal, and intensity bias correction are common pre-processing steps. 2. Pre-processing, image processing methods are used to successfully extract features that represent each unique tissue type. Features like intensity gradients, texture, asymmetry-related features, multifractal Brownian motion features, textons, first order statistical features, and edge-based features are a few examples. 3. Different types of classifiers, including SVM, kNN, Neural Networks (NN), SOM, and RF, are implemented using these attributes. 4. In some instances, segmentation results are improved to improve performance. Among the preferred options are Conditional Random Fields (CRF) and Connected Components (CC).
Deformable Models	Curves or surfaces established within an image domain that are deformable can move in response to both internal forces generated by the model itself and external forces calculated from the image data. The incorporation of prior shape information in deformable models for medical image segmentation frequently increases efficiency.
Mean Shifts	For dampening shade or tone disparities in confined objects, the Mean Shift segmentation is a local homogenization approach. An illustration is worth a thousand words: Replaces every pixel with the average of those in a range-r neighborhood and whose value is within 'a' distance 'd'.
Graph Cuts	You can use the semiautomatic segmentation technique known as "graph cut" to separate the foreground and background components of an image. Good initialization is not necessary for graph cut segmentation. To specify what you want in the foreground and what you want in the background, simply sketch lines on the image.
Dynamic Programming	Due to its globally optimal segmentation method, the dynamic programming (DP) technique has been frequently used in time series segmentation tasks.
Mathematical Morphology	The work of morphological segmentation, which tries to separate words into morphemes that carry meaning, is crucial to the process of processing natural language. Morphological Segmentation is an ImageJ/Fiji plugin that segments grayscale images of any kind (8, 16, and 32-bit) in 2D and 3D using morphological operations like extended minima and morphological gradient.
Thresholding	Thresholding is a sort of image segmentation in which we modify an image's pixel composition to carry out the analysis. Through the process of thresholding, we turn a color or grayscale image into a binary image, or one that is only black and white.
Deep Learning-based	The usual encoder–decoder structure used by deep learning models for segmentation involves an encoder, a bottleneck, and a decoder or upsampling layer. To squeeze data into a bottleneck and create a representation of the input, deep learning models suggest using a combination of convolutional and downsampling blocks. The decoder then reconstructs the input data to create a segment map, highlighting input locations and classifying them. The decoder's final step includes a sigmoid activation that limits the output to a certain range (0,1). Some of the deep learning models used for segmentation are U-Net, V-Net, FCN, GAN, Mask RCNN, etc.

been quite excellent using these algorithms, and so we recommend using them and their modifications to solve various problems. This classification is illustrated in Fig. 8. Conventional approaches can be further classified as Support Vector Machine (SVM) (Hearst et al., 1998), Naive Bayes (Rish, 2001), Neural Network (NN) (Lisboa and Taktak, 2006), K-Nearest Neighbor (K-NN) (Adyapady R and Annappa, 2022), Extreme Learning Machine (ELM) (Huang et al., 2004), Random Forest (RF) (Biau, 2012), Decision Tree (DT) (Zhong, 2016), Logistic Regression (Haifley, 2002), Discriminant Analysis (Dodia et al., 2019), Bagging Classifier (Machová et al., 2006), AdaBoost (Bartlett and Traskin, 2007), and Fuzzy-based (Kuncheva, 2000). Deep Learning based approaches can be further classified as Convolution Neural Network (CNN) (Yamashita et al., 2018), Recurrent Neural Network (RNN) (Lipton et al., 2015), Deep Belief Network (DBN) (Zhang et al., 2018), Deep Neural Network (DNN) (Abiyev and Ma'aitah, 2018), AlexNet (Krizhevsky et al., 2012), CapsuleNet (Sabour et al., 2017), Residual Neural Network (Resnet) (He et al., 2016), Visual Geometry Group (VGG) (Liu and Deng, 2015), Long Short-Term Memory (LSTM) (Greff et al., 2016), and Restricted Boltzmann Machine (RBM) (Fischer and Igel, 2012).

Deep learning based lung nodule detection systems consists of general building blocks of deep learning layers such as convolution, pooling, activation, normalization, flatten, dropout and fully connected or dense layers. A typical deep learning architecture will consists of a combination of these layers with addition or reduction of few other layers. The mathematical formulation of these layers are explained as follows:

The input provided to the deep learning model for deep learning lung cancer detection system will be a medical image which can be a CT scan, MRI scan, X-ray, and so on. In this case, let us consider the input image as a CT scan image f and kernel h. The first layer is the input layer. Followed by this, the higher level features are learnt in the convolution (C) layers.

$$C[m,n] = (f * h)[m,n] = \sum_j \sum_k h[j,k]\, f[m-j, n-k] \tag{1}$$

Where, m and n are the indexes of rows and columns of the result matrix respectively. The indexes of input image is given by j and k. After the convolution operation, the size of the output feature matrix is reduced by a pooling operation. In this layer, the max pooling operation divides the feature map into different regions and then selects the maximum value from the region and then places that in the corresponding place in the output matrix.

Table 4
Different types of feature descriptors used for lung cancer detection.

	Features	Definition
Texture	Entropy	The measure of uncertainity in an image is known as entropy
	Contrast	The local variance of an image is captured by the contrast feature
	Energy	The sum of squared elements gives the energy of the image
	Homogeneity	The measure of closeness of the distribution of elements in an image is given by homogeneity
Spatial	Angle	The main direction in which the image exists is given by Angle
	Area	The area of the region covering the pixels of an image is given
	Box area	A bounding box of a particular region in an image is given by box area
Gradient	Skewness	Skewness is a measure of the probability distribution asymmetry of a real-value random variable relative to its mean
	Average	A filtering method used for smoothing images by reducing the intensity variation in between pixels in the same neighborhood
	Standard deviation	The measure of variability is given by standard deviation
	Kurtosis	The relative peakedness or flatness of a distribution is given by kurtosis
Radiomics	Co-occurrence features	The spatial based gray level intensities within an image is given by Gray level co-occurrence matrix (GLCM)
	Run-length based features	The number of contiguous voxels having same gray level value and also the run lengths of various intensities in any-direction is given by Gray level run length matrix (GLRL)
	NGTDM based features	Based on the visual representations of an image, a texture analysis method Neighborhood gray tone difference matrix (NGTDM) can be applied on medical images.
Geometrical	Solidity	Solidity can be defined as the area of a particle which is divided by its convex hull area
	Equivalent diameter	The diameter is estimated using Euclidean distance
	Spherical disproportion	The spherical disproportion can be said as inverse of sphericity. The ratio of surface area of the tumor region to the surface area of a sphere is known as spherical disproportion.
	Perimeter	In an image, the distance around the outside of a shape is known as perimeter
	Roundness	The circularity index or irregularity index provides an output 1 if the shape is only circle, and less than 1 for any other shape
	Eccentricity	The eccentricity can be defined as the ratio of the distance between the foci of the shape and its major axis length
	Centroid	The center of mass of the region is given by centroid
	Convex-area	Number of pixels in an image that specifies a convex-hull is known as convex-area of an image

The output matrix resulted from the pooling operation can be batch normalized to avoid the internal covariate shift problem in the feature matrix values. Batch normalization is performed in three steps as given below:

The first step is to calculate the batch mean and variance of the layers' output as shown in Eqs. (2) and (3).

$$\mu_B = \frac{1}{m}\sum_{i=1}^{m} x_i \tag{2}$$

$$\sigma_B^2 = \frac{1}{m}\sum_{i=1}^{m}(x_i - \mu_b)^2 \tag{3}$$

The second step is to normalize the inputs of the layers by previously calculated batch statistics as shown in Eq. (4).

$$\bar{x}_i = \frac{x_i - \mu_B}{\sqrt{\sigma_B^2 - \epsilon}} \tag{4}$$

The third step is to perform scale and shift operation to achieve the layers' output as shown in Eq. (5).

$$y_i = \sqrt{x_i} + \beta \tag{5}$$

Where, β is learned during the training along with other trainable parameters.

The flatten layer is used to bring all the values in the feature matrix into a vector and then is fed to the fully connected layers which consists of neurons. This layer is also called dense layer. A regularization operation is carried out after dense layer, which is dropout layer. In this layer, the neurons are randomly dropped while training. This is done to avoid overfitting issue of the network. The values of this layer is fed to the activation function. If binary classification, sigmoid activation function is used. This returns a value between the range [0,1]. If the value is below 0.5, the sample is assigned to class 1, else to class 2. If multiclass classification, softmax activation function is used. This returns probability values and the class that is assigned with highest probability value, the input sample is assigned to that class.

4. Literature review

The research in the detection of the pulmonary nodule in the lungs has been a challenging problem for decades. The task of building an automatic system that is both reliable and accurate is quite difficult. This section covered a variety of current publications on the detection and classification of lung cancer nodules. Major databases like Google Scholar, IEEE Xplore, PubMed, Web of Science, and Scopus were used to retrieve the papers. The papers were selected from top

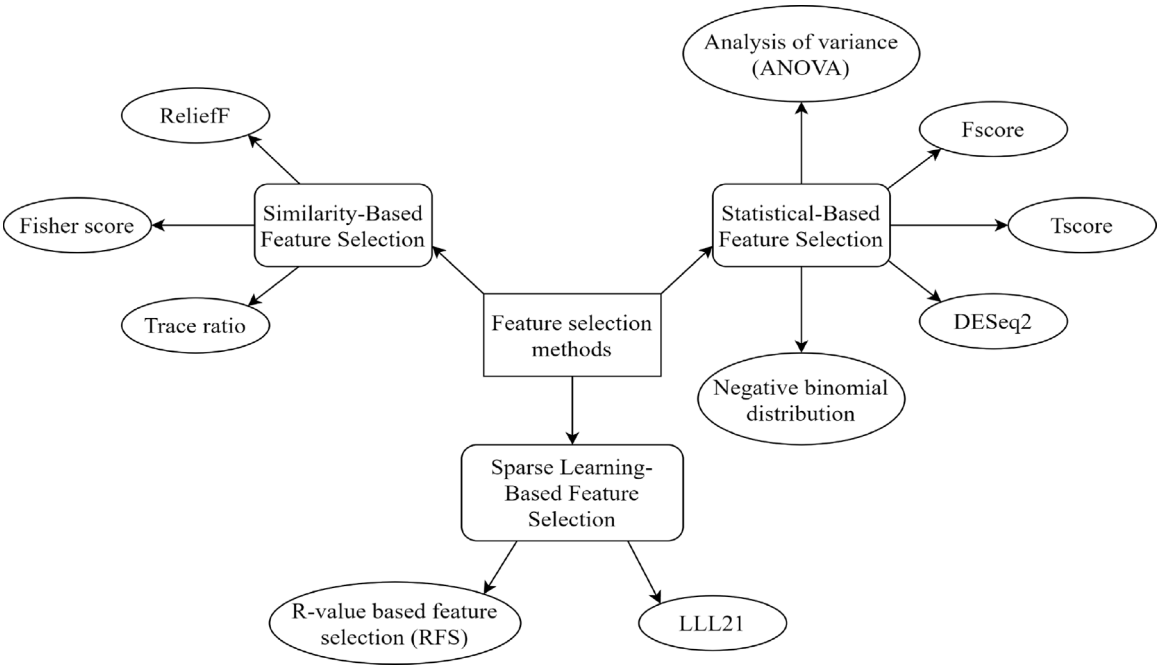

Fig. 7. Feature selection algorithms used for selecting best features to perform lung cancer nodule detection and classification.

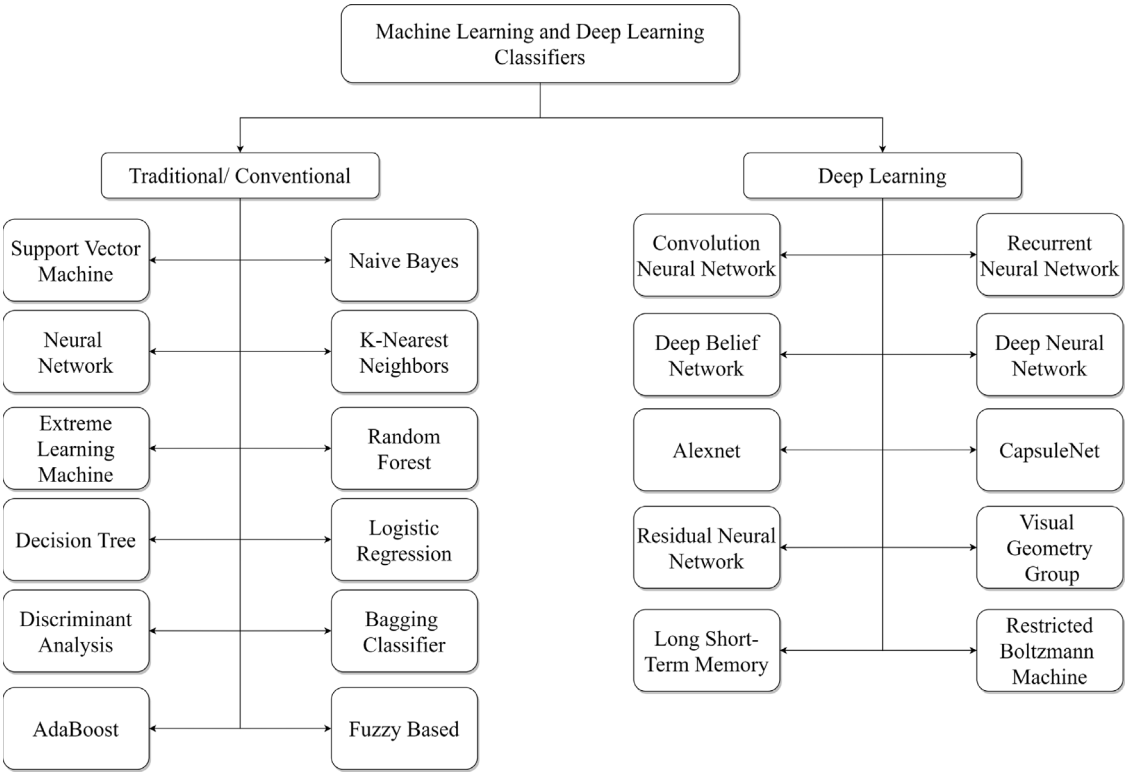

Fig. 8. Categorization of machine learning and deep learning-based classifiers.

tier conferences, journals with SCI, SCIE, and Scopus indexes. The literary work referred in the review are searched by providing keywords such as "lung cancer", "CAD", "tumor detection", "nodule classification", "feature extraction for lung cancer identification", "nodule segmentation", "benign and malignant nodule", "nodule detection", "pulmonary nodule identification", "machine learning", "deep learning", "computer-aided diagnosis", and "artificial intelligence" were used to search the literature. The search terms used to find the articles were similar to those used to find previous research on lung cancer.

The review in our work focuses on deep learning methods for lung cancer nodule detection or segmentation. Deep learning based 55 relevant works have been considered. Table 5 provides a brief discussion of popular deep learning architectures used to segment and classify lung cancer nodules. Table content includes the authors' name, year of publication, the dataset used by authors, methods used, performance

Table 5
Comparison of various deep learning CAD systems for lung cancer based on techniques used and performance achieved.

Authors	Dataset(s) used	Techniques used	Performance measures	Advantages	Limitations
Hua et al. (2015)	LIDC	Deep belief network and Convolutional neural network	Sensitivity=73.4%, Specificity=82.2% (DBN) and Sensitivity=73.3%, Sensitivity= 78.7% (CNN)	First work to apply deep learning techniques to the issue of classifying pulmonary nodules	The main drawback of the deep learning techniques used in this study lies in the question of resizing the input images, resulting in lower sensitivity in both DL techniques
Wang et al. (2018)	LIDC	Histogram of Oriented Gradients (HOG), Local Binary Pattern (LBP), Hybrid CNN network model	Receiver operating characteristic curve (AUC) from 0.9441 to 0.9702	The results achieved are good	The model used for the classification is a complex model and is computationally expensive
Tajbakhsh and Suzuki (2017)	Low-dose thoracic helical CT (LDCT)	massive-training artificial neural networks (MTANNs)	Accuracy=88.06%	A comparison between massive-training ANN and deep convolutional neural network is given	The model's accuracy is lower and can be enhanced by network optimization
Kasinathan et al. (2019)	LIDC	Multiscale Gaussian distribution to smoothen CT images, Enhanced Convolutional Neural Network (CNN)	Accuracy= 97%, Sensitivity= 89%, Specificity= 91%	Accuracy is improved, and model takes less computation time	Increasing the sensitivity also increased false positives
Kumar et al. (2015)	LIDC	Deep features extracted from an autoencoder, Binary decision tree as a classifier	Accuracy=75.01%, Sensitivity=83.35%, and False positive=0.39/patient	False positive rate is reduced and the deep features take into account not only the different traditional semantic characteristics such as lobulation, spiculation, etc., but also the relation between them	However, the accuracy reported is less for the model to be deployed in a hospital environment
Zhao et al. (2018)	LIDC	A hybrid CNN of LeNet and AlexNet	Area under the curve (AUC)= 0.822 to 0.877	The impacts of kernel size, learning rate, batch size preparation, dropout and weight initialization on pulmonary nodule classification CT images were investigated using new Agile CNN	Both used architectures such as LeNet and AlexNet are designed for color images, whereas medical pictures are gray-scale images, making it impossible to make full use of all networks
Liu et al. (2019b)	Private data (60 patients)	Low-level features such as color moment and texture feature, ResNet for classification	Diagnostic accuracy=100% (experimental group) and 74.29% (control group)	The obtained accuracy for diagnostic group is 100%, which is good	However, to check the robustness of model, it would be good if the performance is evaluated on publicly available large data sets such LIDC

(*continued on next page*)

Table 5 (*continued*).

Authors	Dataset(s) used	Techniques used	Performance measures	Advantages	Limitations
Tran et al. (2019)	LUNA	Novel 15-layer 2D deep convolutional neural network architecture	Accuracy=97.2%, Specificity=97.3% and Sensitivity=96%	This novel architecture helped in achieving very good results	The proposed architecture is a 15 layer architecture which needs more computational resources. So, in order to make this model useful to low processing power systems, optimization is required
Hamidian et al. (2017)	LIDC	3D fully convolutional network (FCN)	Sensitivity= 80% and False positives per case= 22.4	A 3-D FCN model is proposed giving a new direction for researchers to explore 3-D CNN	The sensitivity of the model is less and the false positives per case is very high which has to be improved
da Silva et al. (2017)	LIDC	Otsu algorithm, Particle Swarm Optimization (PSO), Genetic algorithm, Convolutional Neural Network	Accuracy=94.78%, Specificity=95.14%, Sensitivity=94.66%, Area under curve=0.949	The results achieved by the model are good	Many preprocessing techniques are applied to the CT scans which in turn increases the overhead of the model and may not be robust
Elnakib et al. (2020)	I-ELCAP	Feature extraction from CNN models such as AlexNet, VGG16 and VGG19; Feature selection using Genetic Algorithm (GA); Classification using K-Nearest Neighbor (KNN), decision trees, and supported vector machines (SVM)	Accuracy= 96.3%, Sensitivity= 97.5%, Specificity= 95%	A CADe system is developed in this work with feature descriptors resulted from deep learning and a pipeline of traditional approaches	As the dataset size is very small, the test set considered is not sufficient to generalize the model's performance
Kim et al. (2016)	In-house data (20 subjects)	Stacked Denoising AutoEncoder (SDAE), linear Support Vector Machine (SVM)	Accuracy= 95.5%, Sensitivity=94.4%, and AUC= 0.987	Data Augmentation is done to balance malignant and benign nodules	Number of subjects are very less to judge the reliability of the model. The model can be further tested on LIDC data
Sun et al. (2017)	LIDC	Convolutional neural network (CNN), deep belief network (DBN), and stacked denoising autoencoder (SDAE)	Area under the curve (AUC)= 0.899 ± 0.018	Three different state-of-art deep neural network architectures have been explored	However, there is still scope for improving the performance of the model
Kasinathan and Jayakumar (2022)	LIDC-IDRI	Cloud-based Lung Tumor Detector and Stage Classifier (Cloud-LTDSC)	Accuracy = 98.6%	The proposed method uses a cloud-based method to identify lung cancer in CT and PET scans	The performance reported in the work is good, however, from 50 images it is not feasible to generalize the method.

(*continued on next page*)

Table 5 (*continued*).

Authors	Dataset(s) used	Techniques used	Performance measures	Advantages	Limitations
Nasrullah et al. (2019)	LUNA16 and LIDC	CMixNet, faster R-CNN, U-Net, and 3D CMixNet and Gradient Boosting Machine (GBM)	Specificity=91% and Sensitivity= 94%	Other than CT scans, clinical biomarkers and physiological symptoms were also considered. A novel 3D deep learning architecture with multiple strategies is proposed.	Training time required is around a week. Also, with such strong 3D networks and various features used the results could be improved
Zhang et al. (2019)	LUNA16	Texture features, shape features, 3D deep DPN features, Gradient boosting machine (GBM) for classification	AUC=0.9687% and Accuracy=93.78%	Relevant features are considered and it helped in yielding good results	Used network is complex and there is still scope for optimization
Ypsilantis and Montana (2016)	LIDC	Thresholding-based region for segmentation, Recurrent Convolutional Networks (ReCTnet) for classification	Sensitivity=90.5%, False positives per scan=4.5	Results from this work suggests that LSTM layers enable to better synthesize the anatomical information across adjacent slices eventually resulting in improved discrimination ability	Having such a deep architecture should not need segmentation as an extra step, as model becomes more complex
Shen et al. (2015)	LIDC	Multi-scale Convolutional Neural Network (MCNN)	Accuracy=86.4%	Multi-scale patches of scans are used rather than segmented patches	The model's efficiency can be enhanced with improved neural network architecture
Rahman et al. (2019)	LIDC	Preprocessed through blurring and thresholding, Classified through MobileNet, VGG- 8 and Inception-v3 deep neural network models	Accuracy=97%, Specificity=97.85% and Sensitivity=96.26%	Model requires low processing power computer, which in turn helps doctor to detect nodules and take better decisions	Images from DICOM format are converted to JPEG format using Microsoft Paint for easy processing, however it looses lot of information
Fu et al. (2017)	LIDC	Thresholding, 2D CNN, SVM Morphological operation, 3D region growing, hand-crafted feature extraction	Sensitivity=89% at False positive= 4/scan and Sensitivity=71.6% at False positive=1/scan	The combination of handcrafted features and CNN features from both lung CT images and enhanced images proves to be a promising method for the identification of lung nodules	When FP/scan is 1, sensitivity is very less making model less efficient
De Carvalho Filho et al. (2018)	LIDC	Otsu algorithm, new indexes of phylogenetic diversity based on topology, CNN	Accuracy=92.63%, Specificity=93.47%, Sensitivity= 90.7% and receiver operating characteristic curve of 0.934	The model performed well given larger number of samples and achieved good results in terms of accuracy, sensitivity, specificity and AUC	There is still scope for improving the sensitivity of the model by performing some modifications in the CNN architecture
Nibali et al. (2017)	LIDC	Deep residual learning, curriculum learning, and transfer learning	Accuracy=89.90%, Specificity=88.64%, Sensitivity= 91.07%, Precision= 89.35 and ROC of 0.9459	Data imbalance of benign and malignant nodules is handled by preprocessing the data	Performance measures like sensitivity and precision can still be improved

(*continued on next page*)

Table 5 (*continued*).

Authors	Dataset(s) used	Techniques used	Performance measures	Advantages	Limitations
Xie et al. (2018)	LIDC	Multi-View Knowledge-based Collaborative (MV-KBC) Deep Learning	AUC=95.70% and Accuracy=91.60%	Results are superior than various state-of-the-art approaches	There are 27 ResNet-50 models embedded in the system. This makes the proposed MV-KBC system require a complex and also high computational power server to train it
Liao et al. (2019)	LUNA16 and the training set of Data Science Bowl 2017	Gaussian filter, 3-D deep neural network	Accuracy=81.42%	Volumetric information is fed to the network and a novel 3-D Convolutional neural network is proposed	There is still scope for enhancing model efficiency
Liu et al. (2018)	LIDC	Novel end-to-end deep learning architecture named dense convolutional binary-tree network (DenseBTNet)	Accuracy=88.31% and Area under curve= 0.9335	A novel deep learning architecture DenseBTNet is proposed	The performance of the model can be improved by optimizing the network and a center crop operation is performed in the architecture which is computationally expensive and may not work for all the cases
Sahu et al. (2018)	LIDC	Lightweight Multi-Section Convolution Neural Network	Accuracy=93.18%	The proposed model is light-weight which makes model to be ported to mobile devices	A cloud-based paradigm is required in which a model uses the capabilities of GPU to quickly determine and retrieve the salient sections
Lakshmanaprabu et al. (2019)	ELCAP	Modified Gravitational Search Algorithm applied to train Optimal Deep Neural Network, Linear Discriminate Analysis (LDA).	Sensitivity=96.2%, Specificity=94.2%, and Accuracy=94.56%	An innovative approach is proposed and is claimed to have speed, also simple to operate, with properties like non-invasive and cheap	The use of 70 images for training and 30 images for testing is too limited for the examination of lung images
Manikandan and Bharathi (2011)	LIDC	Median filter, Convolution Neural Network (CNN)	Accuracy= 96%	Performance of the system is good	Data used for training the model is only 70 images and for testing is 30 images, so the reliability of the model is still a question. It is believed that CNN requires more data to train the network
Bhandary et al. (2020)	LIDC-IDRI	Modified AlexNet, Support Vector Machine	Accuracy = 92.27%	A modified AlexNet is proposed in the work for identifying both lung pneumonia and cancer. The results reported in the paper is good	The approach consists of a pipeline of methods which can be time-consuming for larger datasets.
Zhang and Kong (2020)	LIDC-IDRI	Multi-Scene Deep Learning Framework (MSDLF)	Efficiency= 98.7%	An innovative lung nodule detection scheme was adapted in this method which also reduced the number of False positives	Complexity of the proposed model can be still reduced

(*continued on next page*)

Table 5 (*continued*).

Authors	Dataset(s) used	Techniques used	Performance measures	Advantages	Limitations
Anwer and Ozbay (2020)	Private dataset taken from K1 hospital in Kirkuk, Iraq, some are taken from Frederick Nat. Lab for Cancer Research at the University of Marburg, and Siemens Healthcare.	Convolutional Neural Network	Accuracy= 93.33%, Precision= 92.59%, Recall= 100%	The paper provides a deep learning model CNN for performing lung cancer classification	The model is trained and tested on a private dataset. Also, the number of samples used for training and testing is not available which makes the results not reliable.
Asuntha and Srinivasan (2020)	LIDC dataset	Fuzzy Particle Swarm Optimization CNN (FPSOCNN)	Accuracy= 95.62%, Sensitivity= 97.93%, Specificity= 96.32%	An in-depth analysis of multiple image features such as SIFT, HOG, etc.for performing lung cancer classification is provided in the paper	The paper illustrates wide varieties of feature combination that are used in traditional methods for reducing complexity of CNN model.
da Nóbrega et al. (2018)	LIDC	Features extracted through VGG16, VGG19, InceptionV3, ResNet50, Inception-ResNet-V2, DenseNet169, DenseNet201, NASNetMobile, MobileNet, Xception, NASNetLarge and classified through Naive Bayes, MultiLayer Perceptron , Support Vector Machine , Near Neighbors and Random Forest	Accuracy= 88.41%, AUC=93.19%, F-Score=78.83%, TruePositiveRate= 85.38%, and PositivePredictedvalue= 73.48%	Various models are trained and tested in this work. It is believed that based on the performance and parameters of the models used, it will help researchers to choose a model for their problem	However, the F-Score and positive predicted value are low and can be improved
Setio et al. (2016)	LIDC, ANODE09 challenge and DLCST	Multi-View Convolutional Networks	Sensitivity= 85.4% at 1 false positive per scan and 90.1% at 4 false positives per scan	3 datasets are used for showing the performance of the model	Performance can still be improved, by increasing the sensitivity and reducing the false positives per scan
Jakimovski and Davcev (2019)	Image & Data Archive of the University of South Carolina and the Laboratory of Neuro Imaging (LONI) database	Convolutional Deep Neural Network (CDNN) and a regular CDNN	HighestAccuracy= 99.62% (CDNN), HighestAccuracy= 87.6% (regular CDNN)	The highest result achieved is commendable	The drawback of the model is that the minimal value of certainty is decided manually and is accepted as being satisfactory. Deciding this value by the user, requires lot of domain knowledge, as a single wrong threshold may lead to misclassification

(*continued on next page*)

Table 5 (*continued*).

Authors	Dataset(s) used	Techniques used	Performance measures	Advantages	Limitations
Neal Joshua et al. (2021)	LUNA16	3D AlexNet with lightweight architecture	Accuracy=97.17%	The method uses 3D AlexNet with lightweight architecture implying that model complexity is less as compared to other deep learning models	Authors can extend the work to stage-wise classification of detected malignant nodules
Faruqui et al. (2021)	Medical IoT (MIOT) dataset	LungNet	Accuracy=96.81% FPR = 3.35%	The authors have performed data collection from wearable devices along with latent features extracted from CT scans. The method provides efficient results	However, FPR value is high.
Sori et al. (2021)	Kaggle Data Science Bowl 2017 challenge (KDSB) and LUNA 16	Denoising first two-path convolutional neural network (DFD-Net)	Accuracy=87.8%	An image denoising technique is adapted in this work to improve the performance of the nodule detection task. The method is less complex in terms of computation time	However, accuracy needs to be still improved
Heuvelmans et al. (2021)	NLST	Lung Cancer Prediction Convolutional Neural Network (LCP-CNN)	AUC=94.5% Sensitivity = 99%	The model is used to identify benign and malignant nodules using deep learning methods. The model displayed high sensitivity rates	However, the model has been trained on fewer CT scan images.
Surendar et al. (2021)	LIDC-IDRI	Deep neural network with adaptive sine cosine crow search(DNN-ASCCS)	Accuracy=99.71%	The authors have proposed new segmentation, feature selection and classification methods for lung nodule classification	The results are only reported for less number images which may or may not give similar performance for larger datasets.
Tian et al. (2021)	Lung CT-Diagnosis database	Enhanced Capsule Networks (ECN)	Accuracy= 96.65% Precision = 96.35% Recall = 96.07% F1-score=96.41%	The method uses an optimized fuzzy possibilistic c-ordered mean based algorithm called Converged Search and Rescue (CSAR) and ECN for final diagnosis. The optimization algorithm resulted in promising results	Only 61 patients are considered for training and testing the model making the results less trustworthy
Marentakis et al. (2021)	NSCLC radiomics	Long short-term memory (LSTM) + CNN	Accuracy = 74% AUC = 0.78	The authors have experimented on combinatorial methods to achieve better performance to classify lung cancer histology images. The best results are achieved from the combination of LSTM, CNN, and radiomics	However, the results can be improved.
Feng and Jiang (2022)	Private dataset	Mask RCNN and Dual Path Network (DPN)	Accuracy = 97.94% Sensitivity = 98.12% Specificity = 100%	The results achieved are commendable	The dataset used in the work consists of CT and MRI images of 45 patients, which is less data to generalize the results.

(*continued on next page*)

Table 5 (*continued*).

Authors	Dataset(s) used	Techniques used	Performance measures	Advantages	Limitations
Dodia et al. (2022a)	LUNA16	Elagha initialization-based Fuzzy C-Means clustering (EFCM), BoVW, CNN and SVM	Accuracy=96.87%, Sensitivity=97.15%, and Specificity=96.60%	Results obtained are high and are verified by an expert pulmonologist	Future research can investigate deeper networks with larger datasets and alternative sets of feature representations for lung nodule classification.
Tekade and Rajeswari (2018)	LIDC, LUNA16, Kaggle Data Science Bowl 2017	U-Net, 3-D Multipath VGG-like network	Accuracy=95.60%	Results obtained are appreciable	The networks used are too complex with many parameters. So, there is a scope to optimize the network
Dodia et al. (2022b)	LUNA16	Cauchy Black Widow Optimization based Convolutional Neural Network (CBWO-CNN) and SE-Xception	Level-1 classification accuracy=96.37% and Level-2 classification accuracy=94.75%,	knowledge transfer approach is adapted making it an interesting piece of work with fewer parameters	In the future work, volumetric information can be learned via a 3D model that is constructed and trained utilizing 3D image input.
Kalaivani et al. (2020)	Private dataset	Densely connected convolution neural network (DenseNet) and adaptive boosting algorithm	Accuracy=90.85%	Accuracy obtained is considerable but still needs to be improved	Results are calculated only on 30 images only
Aziz et al. (2022)	Private dataset: 11 anonymous sets of CT images with every set having 300 slices	Multilevel thresholding and Markov Random Field	Accuracy=94.75%, Specificity=99.80%, and Sensitivity=76.34%	This work demonstrates how this approach classifies non-lung in a scan more accurately than lung region. A system's type I error rate is lower when it has a higher specificity.	Average sensitivity being 76.34% is very less for medical imaging applications
Vaiyapuri et al. (2022)	ELCAP Public Lung Image Database	Cat Swarm Optimization-Based Computer-Aided Diagnosis Model	Accuracy= 98.89%	The experimental results showed that the CSO-CADLCC approach outperformed more recent approaches in a variety of measurements	ELCAP dataset contains only 50 images

(*continued on next page*)

Table 5 (*continued*).

Authors	Dataset(s) used	Techniques used	Performance measures	Advantages	Limitations
Selvapandian et al. (2022)	LIDC and TCIA	SCSF-based GAN	Accuracy=94.98%	The suggested approach helps doctors diagnose cancer more accurately and with better analysis	Author claims to improve categorization accuracy by taking into account more data, such as PET in future work
Dodia et al. (2022)	LUNA16	RFR V-Net and NCNet	Sensitivity=98.38% and FPs/Scan=2.3	The proposed NCNet led to significant advancements over current CAD systems	Future work could involve integrating CT images from several sources to extend the dataset because the model overfits for 110 layers.
Althubiti et al. (2022)	41 CT Scans	Ensemble Learning Framework with GLCM Texture Extraction	Accuracy=90.9%	This proposed framework can help doctors and complement current methods in the computer-aided diagnosis of lung cancer	Dataset has very less number of images to generalize results
Riquelme and Akhloufi (2020)	LIDC	U-Net, Faster R-CNN, Mask R-CNN, YOLO, VGG, ResNet,	Accuracy=98%	More datasets and more balanced data can lead to better results is discussed	The implementation of new loss functions, including focal loss, that are intended to address the issue of unbalanced classes, could enhance the current results and aid in more effective training.
Nanglia et al. (2021)	ELCAP lung image dataset	Kernel Attribute Selected Classifier (KASC)	Precision=98.17%, Accuracy=98.08%, Recall=96.5% and F-measure=97%	The obtained performance of the proposed KASC algorithm led to significant advancements in lung cancer classification	The number of CT scans used for training and testing the model for lung cancer classification is very less
Alakwaa et al. (2017)	LUNA16	Deep convolutional neural network (CNN) and U-Net	AUC=0.83	Results achieved for the test set are commendable	The appropriate region where the cancerous nodules are present cannot be estimated using the proposed approach

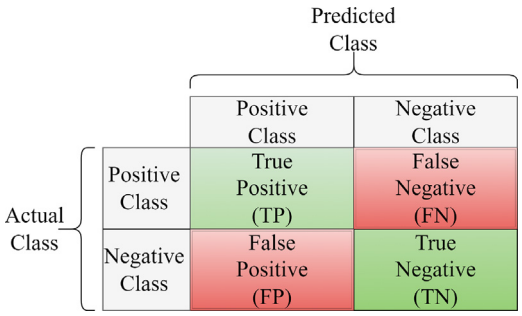

Fig. 9. Confusion matrix to evaluate the performance of a system.

measures, and remarks of the work. This section covers the recent research performed to recognize nodules of lung cancer and distinguish nodules that are benign and malignant to the best of what we know. This review also highlights the comprehensive work carried out by researchers working on medical imaging analysis of lung cancer.

To perform lung cancer nodule detection several methods have been proposed in the recent decade. However, not all the systems are reliable enough to deploy in a real-time environment. Some of the deep methods have resulted in promising performances in terms of evaluation metrics like accuracy, sensitivity, FROC, and so on. The performances that are high amongst the deep learning methods are ensemble CNN and deep learning based segmentation algorithms. The most popular CNN methods resulting in higher performance include combination of two or more conventional CNN model. We can draw a conclusion by this that ensemble methods provide better results as it combines the advantages of two or more networks in order to learn input features in a better way.

5. Performance measures

The next step after the model has been developed is to validate the model. The model's assessment is done by calculating the model's performance using metrics such as accuracy, specificity, sensitivity, precision, recall, F-measure, dice coefficient, Jaccard index, and False positive rate (FPR). The confusion matrix is a table used to measure a system's success in classification. This includes information about classes that are actual and predicted classes. Fig. 9 depicts the confusion matrix used for the performance evaluation of a system. It consists of 2 classes, namely, actual and predicted. Actual is the class to which the sample originally belongs, and predicted is the class in which classifiers predict the sample. It also consists of four output parameters, such as True Positive, True Negative, False Positive, and False Negative. The four output parameters can be explained below:

1. **True Positive (TP):** The sample originally belongs to the positive class and provides the classification result as the positive class. It signifies the number of correct predictions.
   Example: Given nodule is cancerous, and the classifier correctly predicted it as cancerous.
2. **False Negative (FN):** The sample originally belongs to a positive class but is misclassified as a negative class. It signifies the number of incorrect predictions. It is also called as Type 2 error.
   Example: Given nodule is cancerous, and the classifier incorrectly predicted it as non-cancerous.
3. **False Positive (FP):** The sample originally belongs to a negative class and is misclassified as the positive class. The number of incorrect predictions. It is also called as Type 1 error.
   Example: Given nodule is non-cancerous, and the classifier incorrectly predicted it as cancerous.
4. **True Negative (TN):** The sample originally belongs to a negative class, and the classification result is also negative class. This signifies the number of correct predictions.
   Example: Given nodule is non-cancerous, and the classifier correctly predicted it as non-cancerous.

The above mentioned four output parameters are used to calculate the system's important performance measures (metrics). The metrics (Ho, 2019; Ahmed et al., 2019; Hazra et al., 2017; Causey et al., 2019) are described below Table 6 along with the equations.

6. Challenges and future scope

The research in identifying lung cancer nodules using computer-aided algorithms is being performed for three decades. There still exist some challenges that need to be addressed. From a clinical perspective, there are a set of obstacles that can be observed in developing a reliable CAD system. Due to the increased demand for large amounts of data for data-hungry methods like deep learning, the data made available from the providers lack quality assurance, proper annotations, fitness, and correct segmentations. Therefore, one of the important obstacles is that if automated methods are developed for these datasets, the ultimate results may not be accurate. Another reason for not having proper annotations of the data is the multi-dimensionality of the images retrieved. The images generated from a CT scanner can be of 100–400 slices. The more the slices, the higher the data. For an image with more slices, the annotations will be tedious as each slice has to be carefully examined manually by the radiologists. Hence, there is a need for standardized data that has been curated from trained professionals and clinicians. When viewed from an ethical perspective, there is no standard system to check the ethics in which the algorithm is developed. The components in the algorithm can be illegal. The deployment of these algorithms in the hospital environment can cause more harm than good. A law or regulation must be passed to verify the AI algorithms from an ethical perspective.

The current diagnostic's used for lung cancer identification mostly consider only visually recognizable findings from imaging modalities. The presence or absence of lung cancer nodules is solely decided from the images such as chest radiographs, MRI, or CT scans. However, the important factor that needs to be considered is pathological differences observed in the patient along with visually recognizable findings. This can provide an accurate diagnosis of lung cancer. One issue that needs to be addressed is the early diagnosis of the malignant nodules in the patient. The survival rate of the patient can be increased by identifying the malignant nodules at the initial stage of development. Another issue that most developers and researchers often oversee is the type of CT scanners used across the globe. The type of CT scanners varies across the world. In well-developed countries, the CT scanners' configuration is advanced, which can generate CT slices in the image up to 400 or more. However, in developing or under-developed countries, the CT scanners used may not be that advanced. The number of slices taken from the patient may be up to 8 or 16. This huge difference in the number of slices in an image acts as an important drawback that needs to be taken care of when developing a reliable and deployable automated system across the world. Also, the variability of storage formats of the image makes it tedious to build a generalized model. It is also difficult to identify reliable feature representations and integrate them into CAD systems to perform classification of benign and malignant nodules.

In addition, multiple challenges occur in the visibility of the images. The structure of a malignant nodule and a normal pulmonary structure appears to be similar. Because of the difference in the nodule's type and size, distinguishing between cancerous and non-cancerous nodules is complicated. The images that are made available for research purposes are of poor quality and noisy. Therefore, image preprocessing needs to be performed to enhance the visibility of the images.

Many future prospects can be done in developing a better and improved CAD system for lung cancer identification. Khaldi et al.

Table 6
Performance metrics explained with the formula and definition.

Performance metric	Formula	Definition
Accuracy	$Accuracy = \frac{TP+TN}{TP+TN+FP+FN}$	The accuracy measure is to consider the number of correct predictions over the total number of samples. This represents how often the classifier provides the correct output.
Specificity	$Specificity = \frac{TN}{TN+FP}$	It is also called as true negative rate. It is used to calculate the proportion of negatives that are marked as negative.
Sensitivity	$Sensitivity = \frac{TP}{TP+FN}$	It is also called as true positive rate or recall. It is used to measure the number of negatives that are marked as negative.
Precision	$Precision = \frac{TP}{TP+FP}$	It is defined as the fraction of the appropriate samples obtained from the total samples.
Recall	$Recall = \frac{TP}{TP+FN}$	It is the measure of calculating the fragment of the total amount of appropriate samples that are actually retrieved.
F-measure	$F1 = \frac{2 \cdot precision \cdot recall}{precision+recall}$	It is required to calculate both accuracy and recall in order to calculate the F-measure. F-measure is an indicator of test's accuracy.
Dice Coefficient	$DiceCoefficient = \frac{2 \cdot TP}{TP+FP+TP+FN}$	It is used to focus the accuracy in the foreground pixels and penalizes for wrong labels. It is also a validation metric for overlap index and a reproducibility. The dice coefficient value is from 0 to 1, where 0 indicates that there is no spatial overlap, and 1 indicates that there is a complete overlap between binary segmentation results of two sets.
Jaccard Index	$JaccardIndex = \frac{TP}{TP+FN+FP}$	The Jaccard index is also referred to as the Jaccard coefficient of similarity. This metric is used to measure the likeness of two different sets of data. The value is given in the range of 0% to 100%. This compares the samples of two data sets, providing information on how many samples are the same and how many are different.
False Positive Rate	$FalsePositiveRate = \frac{FP}{FP+TN}$	FPR is an important metric used in medical tests. FPR gives an accuracy measure in which it returns a probability value of rejecting the null hypothesis falsely.

(2019) have compared various hand-crafted features and CNN-based texture descriptors that have been mentioned in the literature. The results show that co-occurrence matrix-based descriptors can match or even outperform CNN-based descriptors in their ability to recognize stationary textures. This suggests that suitable hand-crafted features must be chosen for the classification task in conventional algorithms to provide better performance. The recent advent of deep learning has made this task easier as they do not require hand-crafted features for training the classifier. So, there is a lot of scope in deep learning and neural network architectures to build CAD systems for lung cancer identification. In the conventional CAD systems, annotations are quite expensive as it has to be done manually by experienced radiologists. With the help of deep learning, annotation costs can be cut down by automating the annotation process. It can be achieved by training a deep learning model with an extensive data set of annotations. This model can now be used for unseen CT scans' annotation. There is a need for providing clinically relevant explanations for the features discovered by the different learning algorithms as it makes the CAD system more reliable for real-time usage. In the previously developed CAD systems, micronodules (i.e., nodules < 3 mm) are usually truncated at the system's training as it is difficult to detect these sets of nodules. Considering these set of nodules can provide better insight for earlier detection of nodules of lung cancer. The CAD system can be designed in such a way that it learns from both clinical records and medical images for multi-modal analysis. Many authors have considered only a subset of data in the literature, which is not a good practice as it may not be a robust model. In turn, it also affects the performance of the system in realistic scenarios. Hence, there is a need for evaluating CAD systems on larger datasets. More experiments on the larger datasets will provide better performance and generalizability of the systems.

One of the major concerns of developing a fully functional, real-time deployable lung cancer CAD systems is the data imbalance found in the cancerous and non-cancerous nodules in the CT scans and the stage classification of the cancer nodules. Therefore, there is a need to develop a deep learning model which handles data imbalance issue and provides more focus on the cancer nodules present in the CT scans. This can be achieved using attention-based deep learning methods. Also, the low data issue can be temporarily solved using simulated CT scans using augmentation techniques such as Generative Adversarial Networks (GANs). In this current trends, GAN model is gaining more attention to simulate the data which has less number of samples.

Deep models are in general considered to be computationally intensive. Therefore to overcome these issues, in the recent trends, low-complexity deep learning models are used. These models minimizes the additions and multiplications in the neural network training and in turn reduces the overall complexity of the model in both time and space domain. The reason for doing this is to deploy the CAD systems in low-memory devices such as hand-held smart devices, smartphones, etc. This will help the common individual to be aware of the disease condition with the help of professional doctors.

7. Conclusion

The study includes an in-depth analysis of the deep learning algorithms to identify and classify lung cancer nodules. The review provides a brief study of lung cancer. Various datasets are stated that are used predominantly to recognize and diagnose lung cancer. Researchers are provided with an overview and a comparison of various techniques used to diagnose lung cancer. Several approaches and evaluation metrics used to assess the CAD schemes are briefly discussed in the paper with their advantages and limitations. There is a need to develop a better automated and time-tested pulmonary detection system to increment lung cancer patients' life span and detect lung cancer at early stages. The paper concludes by providing the challenges faced in the identification and classification of lung cancer nodules and suggesting probable future research directions.

CRediT authorship contribution statement

Shubham Dodia: Conceptualization, Methodology, Writing – original draft. **Annappa B.:** Supervision, Validation, Writing – review & editing. **Padukudru A. Mahesh:** Investigation, Validation, Writing – review & editing.

Declaration of competing interest

The authors declare that they have no known competing financial interests or personal relationships that could have appeared to influence the work reported in this paper.

Data availability

No data was used for the research described in the article.

References

Abiyev, R., Ma'aitah, M., 2018. Deep convolutional neural networks for chest diseases detection. J. Healthc. Eng. 2018, 1–11. http://dx.doi.org/10.1155/2018/4168538.

Adyapady R, R., Annappa, B., 2022. Micro expression recognition using delaunay triangulation and voronoi tessellation. IETE J. Res. 1–17.

Aerts, H.J., Velazquez, E.R., Leijenaar, R.T., Parmar, C., Grossmann, P., Carvalho, S., Bussink, J., Monshouwer, R., Haibe-Kains, B., Rietveld, D., Hoebers, F., Rietbergen, M.M., Leemans, R., Dekker, A., Quackenbush, J., Gillies, R.J., Lambin, P., 2014. Decoding tumour phenotype by noninvasive imaging using a quantitative radiomics approach. Nature Commun. 5 (1), 1–9.

Aggarwal, T., Furqan, A., Kalra, K., 2015. Feature extraction and LDA based classification of lung nodules in chest CT scan images. In: International Conference on Advances in Computing, Communications and Informatics. ICACCI, IEEE pp. 1189–1193.

Ahmed, S.R.A., Al Barazanchi, I., Mhana, A., Abdulshaheed, H.R., 2019. Lung cancer classification using data mining and supervised learning algorithms on multi-dimensional data set. Period. Eng. Nat. Sci. 7 (2), 438–447.

Al-Tarawneh, M.S., 2012. Lung cancer detection using image processing techniques. Leonardo Electron. J. Pract. Technol. 11 (21), 147–158.

Alakwaa, W., Nassef, M., Badr, A., 2017. Lung cancer detection and classification with 3D convolutional neural network (3D-CNN). Int. J. Adv. Comput. Sci. Appl. 8 (8).

Althubiti, S.A., Paul, S., Mohanty, R., Mohanty, S.N., Alenezi, F., Polat, K., 2022. Ensemble learning framework with GLCM texture extraction for early detection of lung cancer on CT images. Comput. Math. Methods Med. 2022.

Anwer, D.N., Ozbay, S., 2020. Lung cancer classification and detection using convolutional neural networks. In: Proceedings of the 6th International Conference on Engineering &Amp; MIS 2020. pp. 1–8.

Armato, S.G., Hadjiiski, L., Tourassi, G.D., Drukker, K., Giger, M.L., Li, F., Redmond, G., Farahani, K., Kirby, J.S., Clarke, L.P., 2015. SPIE-AAPM-NCI lung nodule classification challenge dataset. The cancer imaging archive.

Asuntha, A., Srinivasan, A., 2020. Deep learning for lung cancer detection and classification. Multimedia Tools Appl. 1–32.

Aziz, K., Saripan, M., Saad, F., Abdullah, R., Waeleh, N., 2022. A Markov random field approach for CT image lung classification using image processing. Radiat. Phys. Chem. 110440.

Baldwin, D.R., 2015. Prediction of risk of lung cancer in populations and in pulmonary nodules: significant progress to drive changes in paradigms. Lung Cancer 1–3. http://dx.doi.org/10.1016/j.lungcan.2015.05.004.

Bartlett, P.L., Traskin, M., 2007. Adaboost is consistent. J. Mach. Learn. Res. 8 (Oct), 2347–2368.

Bhalerao, R.Y., Jani, H.P., Gaitonde, R.K., Raut, V., 2019. A novel approach for detection of lung cancer using digital image processing and convolution neural networks. In: 2019 5th International Conference on Advanced Computing & Communication Systems. ICACCS, IEEE, pp. 577–583.

Bhandary, A., Prabhu, G.A., Rajinikanth, V., Thanaraj, K.P., Satapathy, S.C., Robbins, D.E., Shasky, C., Zhang, Y.-D., Tavares, J.M.R., Raja, N.S.M., 2020. Deep-learning framework to detect lung abnormality–a study with chest X-Ray and lung CT scan images. Pattern Recognit. Lett. 129, 271–278.

Bhavanishankar, K., Sudhamani, M., 2015. Techniques for detection of solitary pulmonary nodules in human lung and their classifications-A survey. Int. J. Cybern. Inf.(IJCI) 4 (1), 27–40.

Biau, G., 2012. Analysis of a random forests model. J. Mach. Learn. Res. 13 (Apr), 1063–1095.

Bray, F., Ferlay, J., Soerjomataram, I., Siegel, R.L., Torre, L.A., Jemal, A., 2018. Global cancer statistics 2018: GLOBOCAN estimates of incidence and mortality worldwide for 36 cancers in 185 countries. CA: Cancer J. Clin. 68 (6), 394–424.

Causey, J.L., Guan, Y., Dong, W., Walker, K., Qualls, J.A., Prior, F., Huang, X., 2019. Lung cancer screening with low-dose CT scans using a deep learning approach. arXiv preprint arXiv:1906.00240.

Chiang, A., Detterbeck, F., Stewart, T., Decker, R., Tanoue, L., 2019. Non-small cell lung cancer. DeVita, Hellman, Rosenberg's Cancer: Princ. Pract. Oncol. 11.

Choi, W., Oh, J.H., Riyahi, S., Liu, C.-J., Jiang, F., Chen, W., White, C., Rimner, A., Mechalakos, J.G., Deasy, J.O., Lu, W., 2018. Radiomics analysis of pulmonary nodules in low-dose CT for early detection of lung cancer. Med. Phys. 45 (4), 1537–1549. http://dx.doi.org/10.1002/mp.12820.

Choromańska, A., Macura, K.J., 2012. Evaluation of solitary pulmonary nodule detected during computed tomography examination. Pol. J. Radiol. 77 (2), 22.

Cieszanowski, A., Lisowska, A., Dabrowska, M., Korczynski, P., Zukowska, M., Grudzinski, I.P., Pacho, R., Rowinski, O., Krenke, R., 2016. MR imaging of pulmonary nodules: detection rate and accuracy of size estimation in comparison to computed tomography. PLoS One 11 (6), e0156272. http://dx.doi.org/10.1371/journal.pone.0156272.

da Silva, G.L., da Silva Neto, O.P., Silva, A.C., de Paiva, A.C., Gattass, M., 2017. Lung nodules diagnosis based on evolutionary convolutional neural network. Multimedia Tools Appl. 76 (18), 19039–19055.

De Carvalho Filho, A.O., Silva, A.C., de Paiva, A.C., Nunes, R.A., Gattass, M., 2018. Classification of patterns of benignity and malignancy based on CT using topology-based phylogenetic diversity index and convolutional neural network. Pattern Recognit. 81, 200–212.

DeSantis, C.E., Miller, K.D., Goding Sauer, A., Jemal, A., Siegel, R.L., 2019. Cancer statistics for African Americans, 2019. CA: Cancer J. Clin. 69 (3), 211–233.

Diciotti, S., Picozzi, G., Falchini, M., Mascalchi, M., Villari, N., Valli, G., 2008. 3-D segmentation algorithm of small lung nodules in spiral CT images. IEEE Trans. Inf. Technol. Biomed. 12 (1), 7–19.

Dodia, S., Annappa, B., Padukudru, M.A., 2022a. A novel artificial intelligence-based lung nodule segmentation and classification system on CT scans. In: International Conference on Computer Vision and Image Processing. Springer, pp. 552–564.

Dodia, S., Annappa, B., Padukudru, M.A., 2022b. A novel bi-level lung cancer classification system on CT scans. In: Annual Conference on Medical Image Understanding and Analysis. Springer, pp. 578–593.

Dodia, S., Basava, A., Padukudru Anand, M., 2022. A novel receptive field-regularized V-net and nodule classification network for lung nodule detection. Int. J. Imaging Syst. Technol. 32 (1), 88–101.

Dodia, S., Edla, D.R., Bablani, A., Ramesh, D., Kuppili, V., 2019. An efficient EEG based deceit identification test using wavelet packet transform and linear discriminant analysis. J. Neurosci. Methods 314, 31–40.

Dolejsi, M., Kybic, J., Polovincak, M., Tuma, S., 2009. The lung time: Annotated lung nodule dataset and nodule detection framework. In: Medical Imaging 2009: Computer-Aided Diagnosis, Vol. 7260. International Society for Optics and Photonics, p. 72601U.

Elnakib, A., Amer, H.M., Abou-Chadi, F.E., 2020. Early lung cancer detection using deep learning optimization. Int. J. Online Biomed. Eng. (IJOE) 16 (06), 82–94.

Farag, A., Elhabian, S., Graham, J., Farag, A., Falk, R., 2010. Toward precise pulmonary nodule descriptors for nodule type classification. 13, pp. 626–633. http://dx.doi.org/10.1007/978-3-642-15711-0_78,

Faruqui, N., Yousuf, M.A., Whaiduzzaman, M., Azad, A., Barros, A., Moni, M.A., 2021. Lungnet: A hybrid deep-CNN model for lung cancer diagnosis using CT and wearable sensor-based medical IoT data. Comput. Biol. Med. 139, 104961.

Feng, J., Jiang, J., 2022. Deep learning-based chest CT image features in diagnosis of lung cancer. Comput. Math. Methods Med. 2022.

Ferlay, J., Soerjomataram, I., Dikshit, R., Eser, S., Mathers, C., Rebelo, M., Parkin, D.M., Forman, D., Bray, F., 2015. Cancer incidence and mortality worldwide: sources, methods and major patterns in GLOBOCAN 2012. Int. J. Cancer 136 (5), E359–E386.

Firmino, M., Morais, A.H., Mendoça, R.M., Dantas, M.R., Hekis, H.R., Valentim, R., 2014. Computer-aided detection system for lung cancer in computed tomography scans: review and future prospects. Biomed. Eng. Online 13 (1), 41.

Fischer, A., Igel, C., 2012. An introduction to restricted Boltzmann machines. In: Iberoamerican Congress on Pattern Recognition. Springer, pp. 14–36.

Fontana, R.S., Sanderson, D.R., Woolner, L.B., Taylor, W.F., Miller, W.E., Muhm, J.R., 1986. Lung cancer screening: the mayo program. J. Occup. Med.: Official Publ. Ind. Med. Assoc. 28 (8), 746–750.

Fotin, S.V., Reeves, A.P., Biancardi, A.M., Yankelevitz, D.F., Henschke, C.I., 2009. A multiscale Laplacian of Gaussian filtering approach to automated pulmonary nodule detection from whole-lung low-dose CT scans. In: Medical Imaging 2009: Computer-Aided Diagnosis, Vol. 7260. International Society for Optics and Photonics, p. 72601Q.

Fotin, S.V., Yankelevitz, D.F., Henschke, C.I., Reeves, A.P., 2019. A multiscale Laplacian of Gaussian (log) filtering approach to pulmonary nodule detection from whole-lung CT scans. arXiv preprint arXiv:1907.08328.

Fu, L., Ma, J., Ren, Y., Han, Y.S., Zhao, J., 2017. Automatic detection of lung nodules: false positive reduction using convolution neural networks and hand-crafted features. In: Medical Imaging 2017: Computer-Aided Diagnosis, Vol. 10134. International Society for Optics and Photonics, p. 101340A.

Gibaldi, A., Barone, D., Gavelli, G., Malavasi, S., Bevilacqua, A., 2015. Effects of guided random sampling of TCCs on blood flow values in CT perfusion studies of lung tumors. Acad. Radiol. 22 (1), 58–69.

Ginneken, B.V., Armato, S.G., Hoop, B.D., Vorst, S.V.A.-V.D., Duindam, T., Niemeijer, M., Murphy, K., Schilham, A., Retico, A., Fantacci, M.E., Camarlinghi, N., Bagagli, F., Gori, I., Hara, T., Fujita, H., Gargano, G., Bellotti, R., Tangaro, S., Bolaños, L., Carlo, F.D., Cerello, P., Cheran, S.C., Torres, E.L., Prokop, M., 2010. Comparing and combining algorithms for computer-aided detection of pulmonary nodules in computed tomography scans: The ANODE09 study. Med. Image Anal. 14 (6), 707–722. http://dx.doi.org/10.1016/j.media.2010.05.005.

Greff, K., Srivastava, R.K., Koutník, J., Steunebrink, B.R., Schmidhuber, J., 2016. LSTM: A search space odyssey. IEEE Trans. Neural Netw. Learn. Syst. 28 (10), 2222–2232.

Grove, O., Berglund, A.E., Schabath, M.B., Aerts, H.J., Dekker, A., Wang, H., Velazquez, E.R., Lambin, P., Gu, Y., Balagurunathan, Y., Eikman, E., Gatenby, R., Eschrich, S., Gillies, R., 2015. Quantitative computed tomographic descriptors associate tumor shape complexity and intratumor heterogeneity with prognosis in lung adenocarcinoma. PLoS One 10 (3), e0118261.

Haifley, T., 2002. Linear logistic regression: An introduction. In: IEEE International Integrated Reliability Workshop Final Report, 2002. IEEE, pp. 184–187.

Hamidian, S., Sahiner, B., Petrick, N., Pezeshk, A., 2017. 3D convolutional neural network for automatic detection of lung nodules in chest CT. In: Medical Imaging 2017: Computer-Aided Diagnosis, Vol. 10134. International Society for Optics and Photonics, 1013409.

Hazra, A., Bera, N., Mandal, A., 2017. Predicting lung cancer survivability using SVM and logistic regression algorithms. Int. J. Comput. Appl. 975, 8887.

He, K., Zhang, X., Ren, S., Sun, J., 2016. Deep residual learning for image recognition. In: Proceedings of the IEEE Conference on Computer Vision and Pattern Recognition. pp. 770–778.

Hearst, M.A., Dumais, S.T., Osuna, E., Platt, J., Scholkopf, B., 1998. Support vector machines. IEEE Intell. Syst. Appl. 13 (4), 18–28.

Heuvelmans, M.A., van Ooijen, P.M., Ather, S., Silva, C.F., Han, D., Heussel, C.P., Hickes, W., Kauczor, H.-U., Novotny, P., Peschl, H., et al., 2021. Lung cancer prediction by deep learning to identify benign lung nodules. Lung Cancer 154, 1–4.

Ho, L., 2019. Fully automated GrowCut-based segmentation of melanoma in dermoscopic images. J. Young Investig. 36 (2).

Hollings, N., Shaw, P., 2002. Diagnostic imaging of lung cancer. Eur. Respir. J. 19 (4), 722–742.

Hua, K.L., Hsu, C.H., Hidayati, S.C., Cheng, W.H., Chen, Y.J., 2015. Computer-aided classification of lung nodules on computed tomography images via deep learning technique. OncoTargets Therapy 8.

Huang, S.C., Pareek, A., Zamanian, R., Banerjee, I., Lungren, M.P., 2020. Multimodal fusion with deep neural networks for leveraging CT imaging and electronic health record: a case-study in pulmonary embolism detection. Sci. Rep. 10 (1), 1–9.

Huang, G.-B., Zhu, Q.-Y., Siew, C.-K., 2004. Extreme learning machine: A new learning scheme of feedforward neural networks. In: 2004 IEEE International Joint Conference on Neural Networks (IEEE Cat. No.04CH37541), Vol. 2. pp. 985–990.

Jakimovski, G., Davcev, D., 2019. Using double convolution neural network for lung cancer stage detection. Appl. Sci. 9 (3), 427.

Javaid, M., Javid, M., Rehman, M.Z.U., Shah, S.I.A., 2016. A novel approach to CAD system for the detection of lung nodules in CT images. Comput. Methods Programs Biomed. 135, 125–139.

John, J., Mini, M., 2016. Multilevel thresholding based segmentation and feature extraction for pulmonary nodule detection. Proc. Technol. 24, 957–963.

Kalaivani, N., Manimaran, N., Sophia, S., Devi, D., 2020. Deep learning based lung cancer detection and classification. In: IOP Conference Series: Materials Science and Engineering, Vol. 994. (1), IOP Publishing, 012026.

Kao, Y.S., Yang, J., 2022. Deep learning-based auto-segmentation of lung tumor PET/CT scans: A systematic review. Clin. Transl. Imag. 1–7.

Kasinathan, G., Jayakumar, S., 2022. Cloud-based lung tumor detection and stage classification using deep learning techniques. BioMed Res. Int. 2022.

Kasinathan, G., Jayakumar, S., Gandomi, A.H., Ramachandran, M., Fong, S.J., Patan, R., 2019. Automated 3-D lung tumor detection and classification by an active contour model and CNN classifier. Expert Syst. Appl. 134, 112–119.

Khaldi, B., Aiadi, O., Kherfi, M.L., 2019. Combining colour and grey-level co-occurrence matrix features: A comparative study. IET Image Process. 13 (9), 1401–1410.

Kim, B.C., Sung, Y.S., Suk, H.I., 2016. Deep feature learning for pulmonary nodule classification in a lung CT. In: 2016 4th International Winter Conference on Brain-Computer Interface. BCI, IEEE, pp. 1–3.

Krizhevsky, A., Sutskever, I., Hinton, G.E., 2012. Imagenet classification with deep convolutional neural networks. In: Advances in Neural Information Processing Systems. pp. 1097–1105.

Kulkarni, A., Panditrao, A., 2014. Classification of lung cancer stages on CT scan images using image processing. In: 2014 IEEE International Conference on Advanced Communications, Control and Computing Technologies. IEEE, pp. 1384–1388.

Kumar, A., Fulham, M., Feng, D., Kim, J., 2019. Co-learning feature fusion maps from PET-CT images of lung cancer. IEEE Trans. Med. Imaging 39 (1), 204–217.

Kumar, D., Wong, A., Clausi, D.A., 2015. Lung nodule classification using deep features in CT images. In: 2015 12th Conference on Computer and Robot Vision. IEEE pp. 133–138.

Kuncheva, L.I., 2000. How good are fuzzy if-then classifiers? IEEE Trans. Syst. Man Cybern. B 30 (4), 501–509.

Kuruvilla, J., Gunavathi, K., 2014. Lung cancer classification using neural networks for CT images. Comput. Methods Programs Biomed. 113 (1), 202–209.

Kvale, P.A., Johnson, C.C., Tammemägi, M., Marcus, P.M., Zylak, C.J., Spizarny, D.L., Hocking, W., Oken, M., Commins, J., Ragard, L., Hu, P., Berg, C., Prorok, P., 2014. Interval lung cancers not detected on screening chest X-rays: How are they different? Lung Cancer 86 (1), 41–46. http://dx.doi.org/10.1016/j.lungcan.2014.07.013.

Lakshmanaprabu, S., Mohanty, S.N., Shankar, K., Arunkumar, N., Ramirez, G., 2019. Optimal deep learning model for classification of lung cancer on CT images. Future Gener. Comput. Syst. 92, 374–382.

Lakshmi Narayanan, A., Jeeva, J.B., 2015. A computer aided diagnosis for detection and classification of lung nodules. In: 2015 IEEE 9th International Conference on Intelligent Systems and Control. ISCO, pp. 1–5.

Lavanya, M., P., M.K., 2018. Lung cancer segmentation and diagnosis of lung cancer staging using MEM (modified expectation maximization) algorithm and artificial neural network fuzzy inference system (ANFIS). Biomed. Res. 29, 2919–2924. http://dx.doi.org/10.4066/biomedicalresearch.29-18-740.

Lei, Y., Zhang, J., Shan, H., 2021. Strided self-supervised low-dose CT denoising for lung nodule classification. Phenomics 1 (6), 257–268.

Liao, F., Liang, M., Li, Z., Hu, X., Song, S., 2019. Evaluate the malignancy of pulmonary nodules using the 3-D deep leaky noisy-OR network. IEEE Trans. Neural Netw. Learn. Syst. 30 (11), 3484–3495.

Lipton, Z.C., Berkowitz, J., Elkan, C., 2015. A critical review of recurrent neural networks for sequence learning. arXiv preprint arXiv:1506.00019.

Lisboa, P.J., Taktak, A.F., 2006. The use of artificial neural networks in decision support in cancer: A systematic review. Neural Netw. 19 (4), 408–415. http://dx.doi.org/10.1016/j.neunet.2005.10.007.

Liu, J., Cao, L., Akin, O., Tian, Y., 2019a. Accurate and robust pulmonary nodule detection by 3D feature pyramid network with self-supervised feature learning. arXiv preprint arXiv:1907.11704.

Liu, S., Deng, W., 2015. Very deep convolutional neural network based image classification using small training sample size. In: 2015 3rd IAPR Asian Conference on Pattern Recognition. ACPR, IEEE, pp. 730–734.

Liu, Y., Hao, P., Zhang, P., Xu, X., Wu, J., Chen, W., 2018. Dense convolutional binary-tree networks for lung nodule classification. IEEE Access 6, 49080–49088.

Liu, Y., Wang, H., Gu, Y., Lv, X., 2019b. Image classification toward lung cancer recognition by learning deep quality model. J. Vis. Commun. Image Represent. 63, 102570. http://dx.doi.org/10.1016/j.jvcir.2019.06.012.

Machová, K., Barcak, F., Bednár, P., 2006. A bagging method using decision trees in the role of base classifiers. J. Acta Polytech. Hung. 3 (2), 121–132.

Mahesh, P., Archana, S., Jayaraj, B.S., Patil, S., Chaya, S., Shashidhar, H.P., Sunitha, B., Prabhakar, A.K., 2012. Factors affecting 30-month survival in lung cancer patients. Indian J. Med. Res..

Manikandan, T., Bharathi, N., 2011. Lung cancer diagnosis from CT images using fuzzy inference system. In: International Conference on Computational Intelligence and Information Technology. Springer, pp. 642–647.

Marentakis, P., Karaiskos, P., Kouloulias, V., Kelekis, N., Argentos, S., Oikonomopoulos, N., Loukas, C., 2021. Lung cancer histology classification from CT images based on radiomics and deep learning models. Med. Biol. Eng. Comput. 59 (1), 215–226.

McNitt-Gray, M.F., Armato III, S.G., Meyer, C.R., Reeves Anthony, P., McLennan, G., Pais, R.C., Freymann, J., Brown, M.S., Engelmann, R.M., Bland, P.H., Laderach, G.E., Chris, P., Junfeng, G., Zaid, T., David, P., Qing, Y., David, F.Y., Denise, R.A., Beek, E.J.V., Heber, M., Kazerooni, E.A., Croft, B.Y., Clarke, L.P., 2007. The lung image database consortium (LIDC) data collection process for nodule detection and annotation. Acad. Radiol. 14 (12), 1464–1474.

Monkam, P., Qi, S., Ma, H., Gao, W., Yao, Y., Qian, W., 2019. Detection and classification of pulmonary nodules using convolutional neural networks: A survey. IEEE Access 7, 78075–78091.

Morris, M.A., Saboury, B., Burkett, B., Gao, J., Siegel, E.L., 2018. Reinventing radiology: big data and the future of medical imaging. J. Thoracic Imaging 33 (1), 4–16.

Nair, G.S., D., D.A., 2016. Automated lung nodule detection method for surgical preplanning. International Journal of Research in Engineering and Science 4, 24–29.

Nanglia, P., Kumar, S., Mahajan, A.N., Singh, P., Rathee, D., 2021. A hybrid algorithm for lung cancer classification using SVM and neural networks. ICT Express 7 (3), 335–341.

Nasrullah, N., Sang, J., Alam, M.S., Mateen, M., Cai, B., Hu, H., 2019. Automated lung nodule detection and classification using deep learning combined with multiple strategies. Sensors 19 (17), 3722.

Nazir, I., Haq, I.U., Khan, M.M., Qureshi, M.B., Ullah, H., Butt, S., 2021. Efficient pre-processing and segmentation for lung cancer detection using fused CT images. Electronics 11 (1), 34.

Neal Joshua, E.S., Bhattacharyya, D., Chakkravarthy, M., Byun, Y.-C., 2021. 3D CNN with visual insights for early detection of lung cancer using gradient-weighted class activation. J. Healthcare Engineering 2021.

Nemade, B., 2016. Advanced computerized scheme for detection of lung nodules by incorporating VDE image. International Journal of Innovative Research in Electrical, Electronics, Instrumentation and Control Engineering 4, 54–57.

Ng, Q.S., Goh, V., 2010. Angiogenesis in non-small cell lung cancer: imaging with perfusion computed tomography. J. Thoracic Imaging 25 (2), 142–150.

Nibali, A., He, Z., Wollersheim, D., 2017. Pulmonary nodule classification with deep residual networks. International Journal of Computer Assisted Radiology and Surgery 12 (10), 1799–1808.

Niranjana, G., Ponnavaikko, M., 2017. A review on image processing methods in detecting lung cancer using CT images. In: 2017 International Conference on Technical Advancements in Computers and Communications. ICTACC, IEEE pp. 18–25.

da Nóbrega, R.V.M., Peixoto, S.A., da Silva, S.P.P., Rebouças Filho, P.P., 2018. Lung nodule classification via deep transfer learning in CT lung images. In: 2018 IEEE 31st International Symposium on Computer-Based Medical Systems. CBMS, IEEE, pp. 244–249.

Novo, J., Gonçalves, L., Mendonça, A.M., Campilho, A., 2015. 3D lung nodule candidate detection in multiple scales. In: 2015 14th IAPR International Conference on Machine Vision Applications. MVA, IEEE, pp. 61–64.

Pedrosa, J., Aresta, G., Ferreira, C., Rodrigues, M., Leitão, P., Carvalho, A.S., Rebelo, J., Negrão, E., Ramos, I., Cunha, A., et al., 2019. Lndb: A lung nodule database on computed tomography. arXiv preprint arXiv:1911.08434.

Potghan, S., Rajamenakshi, R., Bhise, A., 2018. Multi-layer perceptron based lung tumor classification. In: 2018 Second International Conference on Electronics, Communication and Aerospace Technology. ICECA, IEEE, pp. 499–502.

Qin, R., Wang, Z., Jiang, L., Qiao, K., Hai, J., Chen, J., Xu, J., Shi, D., Yan, B., 2020. Fine-grained lung cancer classification from PET and CT images based on multidimensional attention mechanism. Complexity 2020.

Rahman, M.S., Shill, P.C., Homayra, Z., 2019. A new method for lung nodule detection using deep neural networks for CT images. In: 2019 International Conference on Electrical, Computer and Communication Engineering. ECCE, IEEE, pp. 1–6.

Rajan, J.R., Chelvan, A.C., Duela, J.S., 2019. Multi-class neural networks to predict lung cancer. J. Med. Syst. 43 (7), 211.

Riquelme, D., Akhloufi, M.A., 2020. Deep learning for lung cancer nodules detection and classification in CT scans. Ai 1 (1), 28–67.

Rish, I., 2001. An empirical study of the Naïve Bayes classifier. In: IJCAI 2001 Workshop on Empirical Methods in Artificial Intelligence, Vol. 3. pp. 41–46.

Robles, A., Harris, C., 2017. Lung cancer field cancerization: Implications for screening by low-dose computed tomography. JNCI: J. National Cancer Inst. 109, http://dx.doi.org/10.1093/jnci/djw328.

Sabour, S., Frosst, N., Hinton, G.E., 2017. Dynamic routing between capsules. In: Proceedings of Advances in Neural Information Processing Systems. pp. 3856–3866.

Sahu, P., Yu, D., Dasari, M., Hou, F., Qin, H., 2018. A lightweight multi-section CNN for lung nodule classification and malignancy estimation. IEEE J. Biomed. Health Inf. 23 (3), 960–968.

Schmidhuber, J., 2015. Deep learning in neural networks: An overview. Neural Netw. 61, 85–117.

Seeram, E., 2010. Computed tomography: physical principles and recent technical advances. J. Med. Imag. Radiat. Sci. 41 (2), 87–109.

Selvapandian, A., Prabhu S, N., Sivakumar, P., Rao DB, J., 2022. Lung cancer detection and severity level classification using sine cosine sail fish optimization based generative adversarial network with CT images. Comput. J. 65 (6), 1611–1630.

Setio, A.A.A., Ciompi, F., Litjens, G., Gerke, P., Jacobs, C., Van Riel, S.J., Wille, M.M.W., Naqibullah, M., Sánchez, C.I., van Ginneken, B., 2016. Pulmonary nodule detection in CT images: false positive reduction using multi-view convolutional networks. IEEE Trans. Med. Imaging 35 (5), 1160–1169.

Setio, A.A.A., Traverso, A., de Bel, T., Berens, M.S., Bogaard, C.V.D., Cerello, P., Chen, H., Dou, Q., Fantacci, M.E., Geurts, B., Gugten, R.V.D., Heng, P.A., Jansen, B., de Kaste, M.M., Kotov, V., Lin, J.Y.-H., Manders, J.T., nora Mengana, A.S., García-Naranjo, J.C., Papavasileiou, E., Prokop, M., Saletta, M., Schaefer-Prokop, C.M., Scholten, E.T., Scholten, L., Snoeren, M.M., Torres, E.L., Vandemeulebroucke, J., Walasek, N., Zuidhof, G.C., Ginneken, B.V., Jacobs, C., 2017. Validation, comparison, and combination of algorithms for automatic detection of pulmonary nodules in computed tomography images: The LUNA16 challenge. Med. Image Anal. 42, 1–13. http://dx.doi.org/10.1016/j.media.2017.06.015.

Shaziya, H., Shyamala, K., Zaheer, R., 2018. Automatic lung segmentation on thoracic CT scans using U-net convolutional network. In: 2018 International Conference on Communication and Signal Processing. ICCSP, IEEE, pp. 0643–0647.

Shen, W., Zhou, M., Yang, F., Yang, C., Tian, J., 2015. Multi-scale convolutional neural networks for lung nodule classification. In: International Conference on Information Processing in Medical Imaging. Springer, pp. 588–599.

Shi, H., Zhang, N., Wu, X.q., Zhang, Y.D., 2020. Multimodal lung tumor image recognition algorithm based on integrated convolutional neural network. Concurr. Comput.: Pract. Exper. 32 (21), e4965.

Shin, B., Park, S., Hong, J.H., An, H.J., Chun, S.H., Kang, K., Ahn, Y.H., Ko, Y.H., Kang, K., 2019. Cascaded wx: A novel prognosis-related feature selection framework in human lung adenocarcinoma transcriptomes. Front. Genet. 10, 662.

Shiraishi, J., Katsuragawa, S., Ikezoe, J., Matsumoto, T., Kobayashi, T., Komatsu, K.i., Matsui, M., Fujita, H., Kodera, Y., Doi, K., 2000. Development of a digital image database for chest radiographs with and without a lung nodule: receiver operating characteristic analysis of radiologists' detection of pulmonary nodules. Am. J. Roentgenol. 174 (1), 71–74.

Sinha, T., 2018. Tumors: Benign and malignant. Int. J. Cancer Therapy Oncol. 10 (3), 555790.

Sivakumar, S., Chandrasekar, C., 2013. Lung nodule detection using fuzzy clustering and support vector machines. Int. J. Eng. Technol. 5 (1), 179–185.

Sori, W.J., Feng, J., Godana, A.W., Liu, S., Gelmecha, D.J., 2021. DFD-net: lung cancer detection from denoised CT scan image using deep learning. Front. Comput. Sci. 15 (2), 1–13.

Sun, W., Zheng, B., Qian, W., 2017. Automatic feature learning using multichannel ROI based on deep structured algorithms for computerized lung cancer diagnosis. Comput. Biol. Med. 89, 530–539.

Surendar, P., et al., 2021. Diagnosis of lung cancer using hybrid deep neural network with adaptive sine cosine crow search algorithm. J. Comput. Sci. 53, 101374.

Sverzellati, N., Silva, M., Calareso, G., Galeone, C., Marchianò, A., Sestini, S., Sozzi, G., Pastorino, U., 2016. Low-dose computed tomography for lung cancer screening: comparison of performance between annual and biennial screen. Eur. Radiol. 26, 3821–3829. http://dx.doi.org/10.1007/s00330-016-4228-3.

Tajbakhsh, N., Suzuki, K., 2017. Comparing two classes of end-to-end machine-learning models in lung nodule detection and classification: MTANNs vs. CNNs. Pattern Recognit. 63, 476–486.

Tekade, R., Rajeswari, K., 2018. Lung cancer detection and classification using deep learning. In: 2018 Fourth International Conference on Computing Communication Control and Automation. ICCUBEA, IEEE, pp. 1–5.

Thabsheera, A.A., Thasleema, T., Rajesh, R., 2019. Lung cancer detection using CT scan images: A review on various image processing techniques. In: Data Analytics and Learning. Springer, pp. 413–419.

Tian, Q., Wu, Y., Ren, X., Razmjooy, N., 2021. A new optimized sequential method for lung tumor diagnosis based on deep learning and converged search and rescue algorithm. Biomed. Signal Process. Control 68, 102761.

Tran, G.S., Nghiem, T.P., Nguyen, V.T., Luong, C.M., Burie, J.C., 2019. Improving accuracy of lung nodule classification using deep learning with focal loss. J. Healthc. Eng. 2019.

Vaiyapuri, T., Alaskar, H., Parvathi, R., Pattabiraman, V., Hussain, A., 2022. Cat swarm optimization-based computer-aided diagnosis model for lung cancer classification in computed tomography images. Appl. Sci. 12 (11), 5491.

Vignesh, V., Kothavari, K., 2014. Classification and detection of lung nodules using virtual dual energy in CXR images. In: 2014 International Conference on Green Computing Communication and Electrical Engineering. ICGCCEE, IEEE, pp. 1–6.

Wang, H., Zhao, T., Li, L.C., Pan, H., Liu, W., Gao, H., Han, F., Wang, Y., Qi, Y., Liang, Z., 2018. A hybrid CNN feature model for pulmonary nodule malignancy risk differentiation. J. X-Ray Sci. Technol. 26 (2), 171–187.

Xie, Y., Xia, Y., Zhang, J., Song, Y., Feng, D., Fulham, M., Cai, W., 2018. Knowledge-based collaborative deep learning for benign-malignant lung nodule classification on chest CT. IEEE Trans. Med. Imaging 38 (4), 991–1004.

Yamashita, R., Nishio, M., Do, R.K.G., Togashi, K., 2018. Convolutional neural networks: an overview and application in radiology. Insights Into Imaging 9 (4), 611–629.

Ypsilantis, P.-P., Montana, G., 2016. Recurrent convolutional networks for pulmonary nodule detection in CT imaging. arXiv preprint arXiv:1609.09143.

Zhang, Q., Kong, X., 2020. Design of automatic lung nodule detection system based on multi-scene deep learning framework. IEEE Access 8, 90380–90389. http://dx.doi.org/10.1109/ACCESS.2020.2993872.

Zhang, Q., Yang, L.T., Chen, Z., Li, P., 2018. A survey on deep learning for big data. Inf. Fusion 42, 146–157.

Zhang, G., Yang, Z., Gong, L., Jiang, S., Wang, L., 2019. Classification of benign and malignant lung nodules from CT images based on hybrid features. Phys. Med. Biol. 64 (12), 125011. http://dx.doi.org/10.1088/1361-6560/ab2544.

Zhao, X., Liu, L., Qi, S., Teng, Y., Li, J., Qian, W., 2018. Agile convolutional neural network for pulmonary nodule classification using CT images. Int. J. Comput. Assist. Radiol. Surg. 13 (4), 585–595.

Zhao, B., Schwartz, L.H., Kris, M.G., 2015. Data from rider lung ct.(the cancer imaging archive).

Zhong, Y., 2016. The analysis of cases based on decision tree. In: 2016 7th IEEE International Conference on Software Engineering and Service Science. ICSESS, IEEE, pp. 142–147.